PHASE PORTRAITS OF A CLASS OF CONTINUOUS PIECEWISE LINEAR DIFFERENTIAL SYSTEMS

JIE LI[1] AND JAUME LLIBRE[2]

Abstract. In this paper we classify the phase portraits of the class of planar continuous piecewise linear differential systems of the form

$$\dot{x} = a|x| + by + c, \qquad \dot{y} = \alpha|x| + \beta y + \gamma,$$

in the Poincaré disc when $a\beta - b\alpha \neq 0$.

1. Introduction and statement of the main result

Andronov, Vitt and Khaikin [1] started to study the piecewise linear differential systems in the 1920s for modelizing some mechanical systems, but the interest on these kind of differential systems persists up to nowadays. These last twenty years a renewed interest appeared in the mathematical community working in differential systems for understanding the rich dynamics of the piecewise linear differential systems, mainly due to the fact these systems modelize very well many problems coming from mechanics, electronics, economy, ..., look at the survey of Makarenkov and Lamb [10], the books of di Bernardo, Budd, Champneys and Kowalczyk [2], and of Simpson [15], and at the hundreds of references cited in such works. While the phase portraits of the linear differential systems

$$\dot{x} = ax + by + c, \qquad \dot{y} = \alpha x + \beta y + \gamma,$$

are very well known, the phase portrait of the most easiest class of continuous piecewise linear differential systems separated by one straight line (that without loss of generality we can assume that the straight line is $x = 0$)

$$\dot{x} = a|x| + by + c, \qquad \dot{y} = \alpha|x| + \beta y + \gamma, \tag{1}$$

with $a\beta - b\alpha \neq 0$ are unknown. As usual the dot denotes derivative with respect to the independent variable of the differential system, here called the time t. Note that these piecewise linear differential systems are analytic in $\mathbb{R}^2 \setminus \{x = 0\}$ and only continuous on the straight line $x = 0$. Of course the domain of definition of the piecewise linear differential systems (1) is the whole plane $\mathbb{R}^2$.

The objective of this paper is to classify all the topologically distinct phase portraits of the differential systems (1) in the Poincaré disc.

Recall that the *phase portrait* of a differential system is the description of the domain of definition of the differential system as union of all their orbits, in this way we know where born the orbits (i.e. their α-limits), or where they die (i.e. their ω-limits), where are their equilibria, periodic orbits, homoclinic orbits, ..., of course if such kind of orbits exists. In other words the phase portrait of a differential system provides all the qualitative information about the dynamics of a differential system.

A phase portrait in the Poincaré disc has the advantage with respect to a phase portrait in the plane $\mathbb{R}^2$ that it controls the orbits which come from or escape to infinity. Roughly speaking the Poincaré disc $\mathbb{D}$ is the closed disc of radius one centered at the origin of coordinates whose interior has been identified with $\mathbb{R}^2$ and its boundary, the circle $\mathbb{S}^1$, with the infinity of $\mathbb{R}^2$. For more details on the Poincaré disc see subsection 2.2.

2010 *Mathematics Subject Classification.* 34A36, 34C07, 37G05.

Key words and phrases. Continuous piecewise linear differential system; Phase portrait; Poincaré disc.

Our main result is the following one.

Theorem 1. *The phase portrait in the Poincaré disc of a continuous piecewise linear differential system* (1) *is topologically equivalent to one of the* 18 *phase portraits described in Figures 7, 8, 9, 10, 12, 14, 16, 17, 18, 21, 22, 23, 28, 30, 38, 40, 48, 50. Moreover, system* (1) *do not have limit cycles.*

Theorem 1 is proved in sections 3 and 4.

2. Preliminaries

2.1. **The normal forms of the differential systems** (1)**.** The piecewise linear differential system (1) depends on six parameters, but we will see that only two parameters are essential.

Since b and β cannot be zero simultaneously, we can assume that $b \neq 0$ first. Inspired in the Proposition 3.1 of the paper [5] we do the diffeomorphism $h : \mathbb{R}^2 \to \mathbb{R}^2$ defined by $h(x, y) = (x, \beta x - by - c) = (X, Y)$, which transforms system (1) into the piecewise linear differential system

$$\dot{X} = (\beta + a)X - Y, \qquad \dot{Y} = (a\beta - b\alpha)X + (c\beta - b\gamma), \qquad \text{if } X \geq 0, \text{ and} \tag{2}$$

$$\dot{X} = (\beta - a)X - Y, \qquad \dot{Y} = (b\alpha - a\beta)X + (c\beta - b\gamma), \qquad \text{if } X \leq 0. \tag{3}$$

Clearly we can rename the parameters of systems (2) and (3) as follows

$$\dot{X} = \bar{a}X - Y, \qquad \dot{Y} = \bar{d}X + \bar{c}, \qquad \text{if } X \geq 0, \text{ and} \tag{4}$$

$$\dot{X} = \bar{b}X - Y, \qquad \dot{Y} = -\bar{d}X + \bar{c}, \qquad \text{if } X \leq 0, \tag{5}$$

where $\bar{a} = \beta + a$, $\bar{b} = \beta - a$, $\bar{c} = c\beta - b\gamma$ and $\bar{d} = a\beta - b\alpha \neq 0$.

If $\bar{c} = 0$, then doing the rescaling $(X, Y, t) = (x/|d|, y, \bar{t}/|d|)$ systems (4) and (5) become

$$\dot{x} = \hat{a}x - y, \qquad \dot{y} = \pm x, \quad \text{if } x \geq 0, \text{ and}$$

$$\dot{x} = \hat{b}x - y, \qquad \dot{y} = \mp x, \quad \text{if } x \leq 0,$$

where $\hat{a} = \bar{a}/|\bar{d}|$, $\hat{b} = \bar{b}/|\bar{d}|$, now the dot denotes derivative with respect to the new time $\bar{t}$, the upper sign takes place when $\bar{d} > 0$, and the lower sign takes place when $\bar{d} < 0$.

Now we further do the rescaling $(X, Y, t) = (\bar{c}\bar{x}/\bar{d}, \bar{c}\bar{y}/\sqrt{|\bar{d}|}, \bar{t}/\sqrt{|\bar{d}|})$ if $\bar{c}\bar{d} > 0$ and systems (4) and (5) become

$$\dot{\bar{x}} = \tilde{a}\bar{x} \pm \bar{y}, \qquad \dot{\bar{y}} = \bar{x} + 1, \qquad \text{if } \bar{x} \geq 0, \text{ and} \tag{6}$$

$$\dot{\bar{x}} = \tilde{b}\bar{x} \pm \bar{y}, \qquad \dot{\bar{y}} = -\bar{x} + 1, \quad \text{if } \bar{x} \leq 0, \tag{7}$$

where $\tilde{a} = \bar{a}/\sqrt{|\bar{d}|}$, $\tilde{b} = \bar{b}/\sqrt{|\bar{d}|}$, and now the dot denotes derivative with respect to the new time $\bar{t}$. Moreover, if $\bar{d} > 0$ then the signs in (6) and (7) are negative, otherwise they are positive. When $\bar{c}\bar{d} < 0$, using the rescaling $(X, Y, t) = (-\bar{c}\bar{x}/\bar{d}, \bar{c}\bar{y}/\sqrt{|\bar{d}|}, \bar{t}/\sqrt{|\bar{d}|})$, we change systems (4) and (5) to the following

$$\dot{\bar{x}} = \tilde{a}\bar{x} \pm \bar{y}, \qquad \dot{\bar{y}} = -\bar{x} + 1, \qquad \text{if } \bar{x} \geq 0, \text{ and} \tag{8}$$

$$\dot{\bar{x}} = \tilde{b}\bar{x} \pm \bar{y}, \qquad \dot{\bar{y}} = \bar{x} + 1, \quad \text{if } \bar{x} \leq 0. \tag{9}$$

Similarly, if $\bar{d} > 0$ then the signs in (8) and (9) are negative, otherwise they are positive.

Assuming that $b = 0$, we similarly do the diffeomorphism $h : \mathbb{R}^2 \to \mathbb{R}^2$ defined as $h(x, y) = (x, \beta y + \gamma) = (X, Y)$, which transforms system (1) into the piecewise linear differential system

$$\dot{X} = aX + c, \qquad \dot{Y} = \beta(\alpha X + Y), \qquad \text{if } X \geq 0, \text{ and} \tag{10}$$

$$\dot{X} = -aX + c, \qquad \dot{Y} = \beta(-\alpha X + Y), \qquad \text{if } X \leq 0. \tag{11}$$

If $c = 0$, then doing the rescaling $(X, Y, t) = (x, y, \bar{t}/|a|)$ systems (10) and (11) become

$$\dot{x} = \pm x, \qquad \dot{y} = \breve{a}x + \breve{b}y, \quad \text{if } x \geq 0, \text{ and}$$

$$\dot{x} = \mp x, \qquad \dot{y} = -\check{a}x + \check{b}y, \quad \text{if } x \leq 0,$$

where $\check{a} = \alpha\beta/|a|$, $\check{b} = \beta/|a|$, now the dot denotes derivative with respect to the new time $\bar{t}$, the upper sign takes place when $a > 0$, and the lower sign takes place when $a < 0$. Note that $a \neq 0$, otherwise $a\beta - \alpha b = 0$.

If $c \neq 0$, doing the rescaling $(X, Y, t) = (|c|x/|a|, y, \bar{t}/|a|$ systems (10) and (11) become

$$\dot{x} = \pm x \pm 1, \qquad \dot{y} = \check{\check{a}}x + \check{b}y, \qquad \text{if } x \geq 0, \text{ and}$$

$$\dot{x} = \mp x \pm 1, \qquad \dot{y} = -\check{\check{a}}x + \check{b}y, \qquad \text{if } x \leq 0, .$$

where $\check{\check{a}} = \alpha\beta|c|/|a|^2$, $\check{b} = \beta/|a|$ and now the dot denotes derivative with respect to the new time $\bar{t}$. Note that the signs of a and c determine the signs in front of x and 1 respectively. More precisely, the upper signs takes place when $a > 0$ and $c > 0$ respectively, and the lower signs takes place when $a < 0$ and $c < 0$ respectively. This completes the proof of Table 1.

As we shall see in subsection 2.1 to classify the phase portraits of the piecewise differential systems (1) is equivalent to classify the phase portraits of the piecewise linear differential systems of Table 1. Note that piecewise linear differential systems of Table 1 only depend on two parameters.

2.2. **Poincaré compactification.** In the proof of Theorem 1 we will use the Poincaré compactification of a planar polynomial vector field $\mathcal{X}(x, y) = (P(x, y), Q(x, y))$ of degree d. The *Poincaré compactification* of $\mathcal{X}$, denoted by $p(\mathcal{X})$, is an induced vector field on $\mathbb{S}^2 = \{y = (y_1, y_2, y_3) \in \mathbb{R}^3 : y_1^2 + y_2^2 + y_3^2 = 1\}$. We call $\mathbb{S}^2$ the *Poincaré sphere*. For more details on the Poincaré compactification see [3, Chapter 5]. Here we just introduce what will be needed.

Denote by $T_p\mathbb{S}^2$ be the tangent space to $\mathbb{S}^2$ at the point p. Assume that $\mathcal{X}$ is defined in the plane $T_{(0,0,1)}\mathbb{S}^2 = \mathbb{R}^2$. Consider the central projection $f\colon T_{(0,0,1)}\mathbb{S}^2 \to \mathbb{S}^2$. This map defines two copies of $\mathcal{X}$, one in the open northern hemisphere $\mathcal{H}^+$ and the other in the open southern hemisphere $\mathcal{H}^-$. Denote by $\mathcal{X}^1$ the vector field $Df \circ \mathcal{X}$ defined on $\mathbb{S}^2$ except on its equator $\mathbb{S}^1 = \{y \in \mathbb{S}^2 : y_3 = 0\}$. Clearly $\mathbb{S}^1$ is identified to the infinity of $\mathbb{R}^2$. In order to extend $\mathcal{X}^1$ to a vector field on $\mathbb{S}^2$ (including $\mathbb{S}^1$) it is necessary that $\mathcal{X}$ satisfies suitable conditions. In the case that $\mathcal{X}$ is a planar polynomial vector field of degree n then $p(\mathcal{X})$ is the only analytic extension of $y_3^{d-1}\mathcal{X}'$ to $\mathbb{S}^2$. On $\mathbb{S}^2 \setminus \mathbb{S}^1 = \mathcal{H}^+ \cup \mathcal{H}^-$ there are two symmetric copies of $p(\mathcal{X})$, one in $\mathcal{H}^+$ and the other in $\mathcal{H}^-$, and knowing the behaviour of $p(\mathcal{X})$ around $\mathbb{S}^1$, we know the behaviour of $\mathcal{X}$ at infinity. The Poincaré compactification has the property that $\mathbb{S}^1$ is invariant under the flow of $p(\mathcal{X})$. The equilibria of $\mathcal{X}$ are called the *finite equilibria* of $\mathcal{X}$ or of $p(\mathcal{X})$, while the equilibria of $p(\mathcal{X})$ contained in $\mathbb{S}^1$, i.e. at infinity, are called the *infinite equilibria* of $\mathcal{X}$ or of $p(\mathcal{X})$. It is known that the infinity equilibria appear in pairs diametrically opposed.

To study the vector field $p(\mathcal{X})$ we use six local charts on $\mathbb{S}^2$ given by $U_k = \{y \in \mathbb{S}^2 : y_k > 0\}$, $V_k = \{y \in \mathbb{S}^2 : y_k < 0\}$ for $k = 1, 2, 3$. The corresponding local maps $\phi_k : U_k \to \mathbb{R}^2$ and $\psi_k : V_k \to \mathbb{R}^2$ are defined as $\phi_k(y) = -\psi_k(y) = (y_m/y_k, y_n/y_k)$ for $m < n$ and $m, n \neq k$. We denote by $z = (u, v)$ the value of $\phi_k(y)$ or $\psi_k(y)$ for any k, such that (u, v) will play different roles depending on the local chart we are considering. The points of the infinity $\mathbb{S}^1$ in any chart have $v = 0$. The expression for $p(X)$ in local chart (U_1, ϕ_1) is

$$\dot{u} = v^d \left[-uP\left(\frac{1}{v}, \frac{u}{v}\right) + Q\left(\frac{1}{v}, \frac{u}{v}\right) \right], \quad \dot{v} = -v^{d+1}P\left(\frac{1}{v}, \frac{u}{v}\right),$$

in the local chart (U_2, ϕ_2) is

$$\dot{u} = v^d \left[-uQ\left(\frac{u}{v}, \frac{1}{v}\right) + P\left(\frac{u}{v}, \frac{1}{v}\right) \right], \quad \dot{v} = -v^{d+1}Q\left(\frac{u}{v}, \frac{1}{v}\right),$$

and in the local chart (U_3, ϕ_3) is $\dot{u} = P(u, v), \quad \dot{v} = Q(u, v)$.

We note that the expression of the vector field $p(\mathbf{X})$ in the local chart (V_i, ψ_i) is equal to the expression in the local chart (U_i, ϕ_i) multiplied by $(-1)^{d-1}$ for $i = 1, 2, 3$. Observe that the points (u, v) of $\mathbb{S}^1$, i.e. the points identified with the infinity of the plane $\mathbb{R}^2$, in any local chart have its coordinate $v = 0$.

$b \neq 0$	$\bar{c} < 0$	$\bar{d} > 0$	(I):	$S_+ : \dot{x} = \tilde{a}x + y, \quad \dot{y} = -x + 1, \quad \text{if } x \geq 0$ $S_- : \dot{x} = \tilde{b}x + y, \quad \dot{y} = x + 1, \quad \text{if } x \leq 0$
		$\bar{d} < 0$	(II):	$S_+ : \dot{x} = \tilde{a}x - y, \quad \dot{y} = -x + 1, \quad \text{if } x \geq 0$ $S_- : \dot{x} = \tilde{b}x - y, \quad \dot{y} = x + 1, \quad \text{if } x \leq 0$
	$\bar{c} = 0$	$\bar{d} > 0$	(III):	$S_+ : \dot{x} = \hat{a}x - y, \quad \dot{y} = x, \quad \text{if } x \geq 0$ $S_- : \dot{x} = \hat{b}x - y, \quad \dot{y} = -x, \quad \text{if } x \leq 0$
		$\bar{d} < 0$	(IV):	$S_+ : \dot{x} = \hat{a}x - y, \quad \dot{y} = -x, \quad \text{if } x \geq 0$ $S_- : \dot{x} = \hat{b}x - y, \quad \dot{y} = x, \quad \text{if } x \leq 0$
	$\bar{c} > 0$	$\bar{d} > 0$	(V):	$S_+ : \dot{x} = \tilde{a}x - y, \quad \dot{y} = x + 1, \quad \text{if } x \geq 0$ $S_- : \dot{x} = \tilde{b}x - y, \quad \dot{y} = -x + 1, \quad \text{if } x \leq 0$
		$\bar{d} < 0$	(VI):	$S_+ : \dot{x} = \tilde{a}x + y, \quad \dot{y} = x + 1, \quad \text{if } x \geq 0$ $S_- : \dot{x} = \tilde{b}x + y, \quad \dot{y} = -x + 1, \quad \text{if } x \leq 0$
$b = 0$	$c < 0$	$a > 0$	(VII):	$S_+ : \dot{x} = x - 1, \quad \dot{y} = \check{\breve{a}}x + \check{b}y, \quad \text{if } x \geq 0$ $S_- : \dot{x} = -x - 1, \quad \dot{y} = -\check{\breve{a}}x + \check{b}y, \quad \text{if } x \leq 0,$
		$a < 0$	(VIII):	$S_+ : \dot{x} = -x - 1, \quad \dot{y} = \check{\breve{a}}x + \check{b}y, \quad \text{if } x \geq 0$ $S_- : \dot{x} = x - 1, \quad \dot{y} = -\check{\breve{a}}x + \check{b}y, \quad \text{if } x \leq 0,$
	$c = 0$	$a > 0$	(IX):	$S_+ : \dot{x} = x, \quad \dot{y} = \breve{a}x + \check{b}y, \quad \text{if } x \geq 0$ $S_- : \dot{x} = -x, \quad \dot{y} = -\breve{a}x + \check{b}y, \quad \text{if } x \leq 0,$
		$a < 0$	(X):	$S_+ : \dot{x} = -x, \quad \dot{y} = \breve{a}x + \check{b}y, \quad \text{if } x \geq 0$ $S_- : \dot{x} = x, \quad \dot{y} = -\breve{a}x + \check{b}y, \quad \text{if } x \leq 0,$
	$c > 0$	$a > 0$	(XI):	$S_+ : \dot{x} = x + 1, \quad \dot{y} = \check{\breve{a}}x + \check{b}y, \quad \text{if } x \geq 0$ $S_- : \dot{x} = -x + 1, \quad \dot{y} = -\check{\breve{a}}x + \check{b}y, \quad \text{if } x \leq 0,$
		$a < 0$	(XII):	$S_+ : \dot{x} = -x + 1, \quad \dot{y} = \check{\breve{a}}x + \check{b}y, \quad \text{if } x \geq 0$ $S_- : \dot{x} = x + 1, \quad \dot{y} = -\check{\breve{a}}x + \check{b}y, \quad \text{if } x \leq 0,$

TABLE 1. The 12 normal forms with only two parameters of the piecewise differential systems (1).

The orthogonal projection under $\pi(y_1, y_2, y_3) = (y_1, y_2)$ of the closed northern hemisphere of $\mathbb{S}^2$ onto the plane $y_3 = 0$ is a closed disc $\mathbb{D}$ of radius one centered at the origin of coordinates called the *Poincaré disc*. Since a copy of the vector field $\mathbf{X}$ on the plane $\mathbb{R}^2$ is in the open northern hemisphere of $\mathbb{S}^2$, the interior of the Poincaré disc $\mathbb{D}$ is identified with $\mathbb{R}^2$ and the boundary of $\mathbb{D}$, the equator of $\mathbb{S}^2$, is identified with the infinity of $\mathbb{R}^2$. Consequently the phase portrait of the vector field $\mathbf{X}$ extended to the infinity corresponds to the projection of the phase portrait of the vector field $p(\mathbf{X})$ on the Poincaré disc $\mathbb{D}$.

By definition the *infinite equilibria* of the polynomial vector field $\mathbf{X}$ are the equilibria of $p(\mathbf{X})$ contained in the boundary of the Poincaré disc, i.e. in $\mathbb{S}^1$, and the *finite equilibria* of $\mathbf{X}$ are the equilibria of $p(\mathbf{X})$ contained in the interior of the Poincaré disc, which of course coincide with the equilibria of X in $\mathbb{R}^2$.

We remark that the infinite equilibria appear in pairs diametrally opposite on the boundary of the Poincaré disc.

Note that for studying the infinite equilibria of the piecewise differential system (1) in $x \geq 0$ we only need to study the infinite equilibria which are in the local chart U_1 and to determine if the origin of the local chart U_2 is or not an equilibrium. While for studying the infinite equilibria of the piecewise differential system (1) in $x \leq 0$ we only need to study the infinite equilibria which are in the local chart V_1 and to determine if the origin of the local chart U_2 is or not an equilibrium.

2.3. **Topological equivalence of two polynomial vector fields.** Let $\mathbf{X}_1$ and $\mathbf{X}_2$ be two polynomial vector fields on $\mathbb{R}^2$. We say that they are *topologically equivalent* if there exists a homeomorphism on the Poincaré disc $\mathbb{D}$ which preserves the infinity $\mathbb{S}^1$ and sends the orbits of $\pi(p(\mathbf{X}_1))$ to orbits of $\pi(p(\mathbf{X}_2))$, preserving or reversing the orientation of all the orbits.

A *separatrix* of the Poincaré compactification $\pi(p(\mathbf{X}))$ is one of following orbits: all the orbits at the infinity $\mathbb{S}^1$, the finite equilibria, periodic orbits which are isolated in the set of periodic orbits at least by one side, when a periodic orbit is isolated in the set of periodic orbits by both sides it is a limit cycle, and the two orbits at the boundary of a hyperbolic sector at a finite or an infinite equilibria, see for more details on the separatrices [11, 12].

The set of all separatrices of $\pi(p(\mathbf{X}))$, which we denote by $\Sigma_{\mathbf{X}}$, is a closed set (see [12]).

A *canonical region* of $\pi(p(\mathbf{X}))$ is an open connected component of $\mathbb{D} \setminus \Sigma_{\mathbf{X}}$. The union of the set $\Sigma_{\mathbf{X}}$ with an orbit of each canonical region form the *separatrix configuration* of $\pi(p(\mathbf{X}))$ and is denoted by $\Sigma'_{\mathbf{X}}$. We denote the number of separatrices of a phase portrait in the Poincaré disc by S, and its number of canonical regions by R.

Two separatrix configurations $\Sigma'_{\mathbf{X}_1}$ and $\Sigma'_{\mathbf{X}_2}$ are *topologically equivalent* if there is a homeomorphism $h : \mathbb{D} \longrightarrow \mathbb{D}$ such that $h(\Sigma'_{\mathbf{X}_1}) = \Sigma'_{\mathbf{X}_2}$.

According to the following theorem which was proved by Markus [11], Neumann [12] and Peixoto [13], it is sufficient to investigate the separatrix configuration of a polynomial differential system, for determining its global phase portrait.

Theorem 2. *Two Poincaré compactified polynomial vector fields $\pi(p(\mathbf{X}_1))$ and $\pi(p(\mathbf{X}_2))$ with finitely many separatrices are topologically equivalent if and only if their separatrix configurations $\Sigma'_{\mathbf{X}_1}$ and $\Sigma'_{\mathbf{X}_2}$ are topologically equivalent.*

2.4. **Limit cycles.** In 1991-1992 Lum and Chua in [8, 9] conjectured that a continuous piecewise linear differential system in the plane with two pieces separated by one straight line has at most one limit cycle. We note that even in this apparent simple case, only after a difficult analysis it was possible to prove the existence of at most one limit cycle, thus in 1998 this conjecture was proved by Freire, Ponce, Rodrigo and Torres in [4]. Recently, a new an easier proof that at most one limit cycle exists for the continuous piecewise linear differential systems with two pieces separated by one straight line has been done by Llibre, Ordóñez and Ponce in [7].

3. Proof of Theorem 1

The piecewise differential systems (1) with $a\beta - b\alpha \neq 0$ are topologically equivalent to some of the 12 piecewise differential systems of Table 1.

If the x-coordinate of an equilibrium is positive (respectively negative), this equilibrium is *real* (respectively *virtual*) for the differential system S_+. If the x-coordinate of an equilibrium is negative (respectively positive), this equilibrium is *real* (respectively *virtual*) for the differential system S_-. Of course if the x-coordinate of an equilibrium is zero, then this equilibrium is real for both differential systems S_+ and S_-.

3.1. **Phase portraits in the Poincaré disc of system (I).**

System	Conditions	Finite Equilibria	Infinite Equilibria
(I)	(I-1): $\tilde{a} < -2$	P_+(stable node)	p_+(saddle), p_-(unstable node)
		P_-(saddle)	q_+(stable node) q_-(unstable node)
	(I-2): $\tilde{a} = -2$	P_+(stable node)	p(semi-hyperbolic saddle-node),
		P_-(saddle)	q_+(stable node) q_-(unstable node)
	(I-3): $-2 < \tilde{a} < 0$	P_+(stable focus)	
		P_-(saddle)	q_+(stable node) q_-(unstable node)
	(I-4): $\tilde{a} = 0$	P_+(center)	
		P_-(saddle)	q_+(stable node) q_-(unstable node)
	(I-5): $0 < \tilde{a} < 2$	P_+(unstable focus)	
		P_-(saddle)	q_+(stable node) q_-(unstable node)
	(I-6): $\tilde{a} = 2$	P_+(unstable node)	p(semi-hyperbolic saddle-node),
		P_-(saddle)	q_+(stable node) q_-(unstable node)
	(I-7): $\tilde{a} > 2$	P_+(unstable node)	p_+(stable node), p_-(saddle)
		P_-(saddle)	q_+(stable node) q_-(unstable node)

Table 2. The local phase portraits at the finite and infinite equilibria of the piecewise differential system (I).

3.1.1. *The finite equilibria.* Note that the differential system S_+ has the equilibrium $P_+ = (1, -\tilde{a})$. While the differential system S_- has the equilibrium $P_- = \left(-1, \tilde{b}\right)$. Then the equilibrium point P_+ (respectively P_-) is real for the differential system S_+ (respectively S_-).

The eigenvalues of the equilibrium P_+ are $\lambda_- := (\tilde{a} - \sqrt{\tilde{a}^2 - 4})/2$ and $\lambda_+ := (\tilde{a} + \sqrt{\tilde{a}^2 - 4})/2$. So if $\tilde{a} \leq -2$ (respectively $\tilde{a} \geq 2$) then $\lambda_- < \lambda_+ < 0$ (respectively $\lambda_+ > \lambda_- > 0$), implying that P_+ is a stable (respectively an unstable) node. If $-2 < \tilde{a} < 0$ (respectively $0 < \tilde{a} < 2$) then $\lambda_\pm$ are a pair of imaginary eigenvalues with negative (respectively positive) real part, implying that P_+ is a stable (respectively an unstable) focus. If $\tilde{a} = 0$ then $\lambda_\pm$ are a pair of purely imaginary eigenvalues, implying that P_+ is a center.

The eigenvalues of the equilibrium P_- are $\mu_- := (\tilde{b} - \sqrt{\tilde{b}^2+4})/2$ and $\mu_+ := (\tilde{b} + \sqrt{\tilde{b}^2+4})/2$. Clearly, $\mu_- < 0 < \mu_+$, implying that P_- is a saddle.

3.1.2. *The infinite equilibria.* We write the differential system S_+ in the local charts U_1 and U_2. Then in the local chart U_1 system S_+ writes

$$\dot{u} = -1 - \tilde{a}u + v - u^2, \quad \dot{v} = -\tilde{a}v - uv; \tag{12}$$

and in the local chart U_2 becomes

$$\dot{u} = 1 + \tilde{a}u + u^2 - uv, \quad \dot{v} = uv - v^2. \tag{13}$$

We separate the study of the infinite equilibria of system S_+ in three cases.

Case (I1$_+$): $\tilde{a} > 2$ or $\tilde{a} < -2$. Then there are only two infinite equilibria of system S_+ in the local chart U_1, namely $p_\pm = \big((-\tilde{a} \pm \sqrt{\tilde{a}^2-4})/2, 0\big)$ and the origin of the local chart U_2 is not an infinite equilibrium.

The eigenvalues of the equilibrium p_+ are $-\sqrt{\tilde{a}^2-4}$ and $\lambda_p = -(\tilde{a} + \sqrt{\tilde{a}^2-4})/2$. If $\tilde{a} > 2$ then $\lambda_p < 0$, implying that p_+ is a stable node, and if $\tilde{a} < -2$ then $\lambda_p > 0$, implying that p_+ is a saddle.

The eigenvalues of the equilibrium p_- are $\sqrt{\tilde{a}^2-4}$ and $\mu_p = -(\tilde{a} - \sqrt{\tilde{a}^2-4})/2$. If $\tilde{a} > 2$ then $\mu_p < 0$, implying that p_- is a saddle, and if $\tilde{a} < -2$ then $\mu_p > 0$, implying that p_- is an unstable node.

Case (I2$_+$): $\tilde{a} = -2$ and $\tilde{a} = 2$. Then there is only one infinite equilibrium of system S_+ in the local chart U_1, namely $p = (-\tilde{a}/2, 0)$, and the origin O of the local chart U_2 is not an infinite equilibrium. The eigenvalues of the equilibrium p are 0 and $-\tilde{a}/2 \neq 0$. Therefore by [3, Theorem 2.19] the infinite equilibrium p is a semi-hyperbolic saddle-node.

Case (I3$_+$): $-2 < \tilde{a} < 2$. Then system S_+ has no infinite equilibria in the local chart U_1 and at the origin of the local chart U_2.

Again we write the differential system S_- in the local charts V_1 and U_2. Then in the local chart V_1 system S_- writes

$$\dot{u} = 1 - \tilde{b}u + v - u^2, \quad \dot{v} = -\tilde{b}v - uv; \tag{14}$$

and in the local chart U_2 becomes

$$\dot{u} = 1 + \tilde{b}u - u^2 - uv, \quad \dot{v} = -uv - v^2. \tag{15}$$

As we did for the system S_+, there are only two infinite equilibria of system S_- in the local chart V_1, namely $q_\pm = \Big((-\tilde{b} \pm \sqrt{\tilde{b}^2+4})/2, 0\Big)$ and the origin of the local chart U_2 is not an infinite equilibrium.

The eigenvalues of the equilibrium q_+ are $-\sqrt{\tilde{b}^2+4}$ and $\lambda_q = -(\tilde{b} + \sqrt{\tilde{b}^2+4})/2$. Clearly, $\lambda_q < 0$, implying that q_+ is a stable node. The eigenvalues of the equilibrium q_- are $\sqrt{\tilde{b}^2+4}$ and $\mu_q = -(\tilde{b} - \sqrt{\tilde{b}^2+4})/2$. And therefore q_- is an unstable node since $\mu_q > 0$.

In summary from the above discussion, we obtain the results of Table 2.

3.1.3. *The global phase portraits in the Poincaré disc.* We below give a discussion for passing from the local phase portraits from all the finite and infinite equilibria to the global phase portraits in the Poincáre disc.

Note by (12)-(15) that the right hand sides of the equation $\dot{v}$ both have a common factor v, implying that the infinity is invariant, i.e, formed by orbits. Besides, we observe that $\dot{x} = y$ and $\dot{y} = 1$ on the y-axis. Then initiating at points lying on the positive y-axis, all orbits go into the half plane $x \geq 0$ while initiating at points lying in the negative y-axis, all orbits go

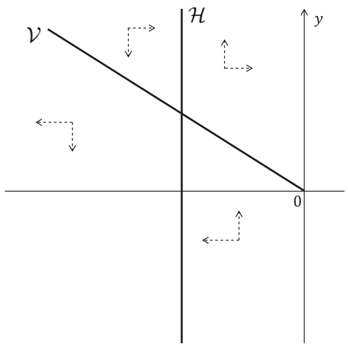

FIGURE 1. $\tilde{b} > 0$

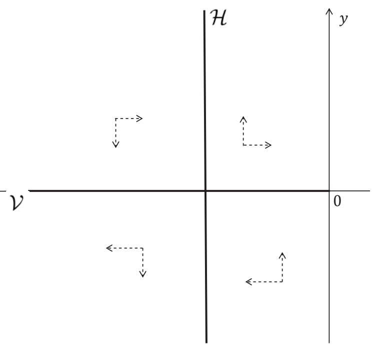

FIGURE 2. $\tilde{b} = 0$

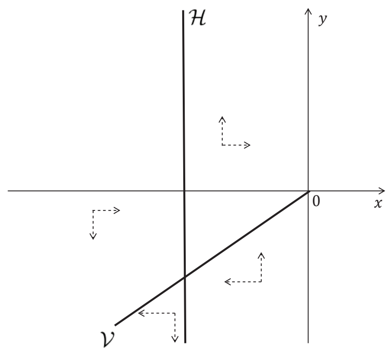

FIGURE 3. $\tilde{b} < 0$

into the half plane $x \leq 0$. On the other hand for system S_- there are the horizontal isocline $\mathcal{H} : x = -1$ and the vertical isocline $\mathcal{V} : y = -\tilde{b}x$. More concretely, we see $\dot{y} > 0$ on the right hand side of $\mathcal{H}$, and $\dot{y} < 0$ on the left hand side of $\mathcal{H}$. And we get $\dot{x} > 0$ in the upper of $\mathcal{V}$, and $\dot{x} < 0$ in the lower of $\mathcal{V}$. So in the four regions divided by $\mathcal{H}$ and $\mathcal{V}$, the vector fields are shown in Figures 1, 2, and 3. According to Table 2, we below discuss the global phase portraits in the following several cases.

In the case (I-1) one stable separatrix of the saddle P_- comes from the unstable node p_- and the second stable separatrix of P_- comes from the unstable node q_-. One unstable separatrix of P_- goes to the stable node q_+ and the second unstable separatrix of P_- goes to the stable node P_+. A stable separatrix of the stable node P_+ comes from the saddle p_+. The remaining orbits of the phase portrait are determined where they start and where they end by the type of stability of the equilibria and by the Poincáre-Bendixson theorem (see for instance theorem 1.25 of [1]). Thus the global phase portrait is given in Figure 7.

In the case (I-2) one stable separatrix of the saddle P_- comes from the unstable node q_- and the second separatrix of P_- comes from the semi-hyperbolic saddle-node p. One unstable separatrix of P_- goes to the stable node q_+ and the second unstable separatrix of P_- goes to the stable node P_+. A stable separatrix of P_+ comes from p. The remaining orbits of the phase portrait are determined where they start and where they end by the type of stability of the equilibria and by the Poincáre-Bendixson theorem. Thus the global phase portrait is given in Figure 8.

In the case (I-3) two stable separatrices of the saddle P_- come from the unstable node q_-. One unstable separatrix of P_- goes to the stable node q_+ and the second unstable separatrix of P_- goes to the stable node P_+. The remaining orbits of the phase portrait are determined by the type of stability of the equilibria and by the Poincáre-Bendixson theorem. Thus the global phase portrait is given in Figure 9,

In the case (I-4) one unstable separatrix of the saddle P_- goes to the stable node q_+ while the other intersects the positive y-axis at $A : (0, y_1)$. On the other hand one stable separatrix of P_- comes from the unstable node q_- while the other intersects the negative y-axis at $A' : (0, y_1')$. Further in the half plane $x \geq 0$, initiating from A, we get an arc intersecting the negative y-axis at $B : (0, y_2)$. Thus there are three situations for position of A': $y_1' > y_2$, $y_1' < y_2$ and $y_1' = y_2$, as shown in Figures 4, 5, and 6. Further we define the two functions

$$H_1(x, y) := (x - 1)^2 + y^2,$$

$$H_2(x, y) := \Big(- \frac{(x+1)\sqrt{4+\tilde{b}^2} - \tilde{b} + \tilde{b}x + 2y}{(x+1)\sqrt{4+\tilde{b}^2} + \tilde{b} - \tilde{b}x - 2y} \Big)^{\tilde{b}} (y^2 - (1+x)^2 + \tilde{b}(xy - \tilde{b}x - y))^{-\sqrt{4+\tilde{b}^2}}.$$

We check H_1 (respectively H_2) is a first integral for system S_+ (respectively S_-), i.e.,

$$(\partial H_1(x, y)/\partial x)y - (\partial H_1(x, y)/\partial y)(1 - x) = 0$$

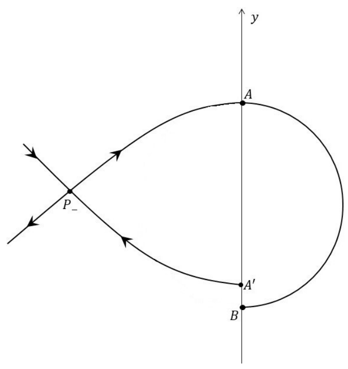

FIGURE 4. $y_1' > y_2$

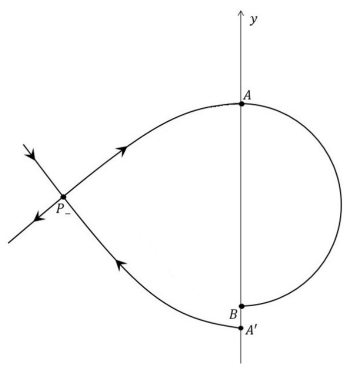

FIGURE 5. $y_1' < y_2$

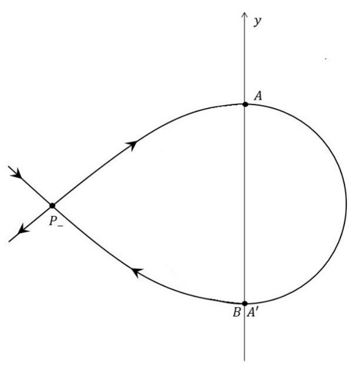

FIGURE 6. $y_1' = y_2$

(respectively $(\partial H_2(x,y)/\partial x)(\tilde{b}x + y) - (\partial H_2(x,y)/\partial y)(x+1) = 0$). Compute

$$H_2(0,0) = (-1)^{-\sqrt{\tilde{b}^2+4}} \left(\frac{\tilde{b} - \sqrt{\tilde{b}^2+4}}{\tilde{b} + \sqrt{\tilde{b}^2+4}} \right)^{\tilde{b}}, \quad \lim_{x \to -1, y \to \tilde{b}} H_2(x,y) = (-1)^{-\sqrt{\tilde{b}^2+4}} \left(\frac{\tilde{b} + \sqrt{\tilde{b}^2+4}}{\tilde{b} - \sqrt{\tilde{b}^2+4}} \right)^{\tilde{b}} \infty.$$

Thus if $y_1' > y_2$ then the unstable separatrix goes though the negative y-axis to the stable node q_+ and the stable separatrix goes around the periodic orbit $\mathcal{C} : (x-1)^2 + y^2 = H_1(0,0) = 1$. If $y_1' < y_2$ then the unstable separatrix goes around $\mathcal{C}$ and the stable separatrix goes though the positive y-axis to the unstable node q_-. On the other hand $\mathcal{C}$ is also a separatrix of the phase portraits for the both situations. The remaining orbits are determined by the type of stability of the equilibria and by the Poincáre-Bendixson theorem. Thus the global phase portraits are shown in Figures 10 and 11 respectively. If $y_1' = y_2$ then the two separatrices coincide, which means that there is a homoclinic orbit linking with the saddle P_-. Clearly some orbits of S_+ intersects y-axis and are symmetric with respect to the x-axis. Thus on the y-axis we look for the values of y such that $H_2(0,y) = H_2(0,-y)$, i.e.,

$$\Big(- \frac{\sqrt{4+b^2} - b + 2y}{\sqrt{4+b^2} + b - 2y} \Big)^b (y^2 - by - 1)^{-\sqrt{4+b^2}} = \Big(- \frac{\sqrt{4+b^2} - b - 2y}{\sqrt{4+b^2} + b + 2y} \Big)^b (y^2 + by - 1)^{-\sqrt{4+b^2}}.$$

The equality holds for any y if $b = 0$. It implies that there are filled with periodic orbits inside the homoclinic orbit. Thus the periodic orbit close to the homoclinic orbit is a separatrix of the phase portrait. The remaining orbits are determined by the Poincáre-Bendixson theorem and by the type of stability of the equilibria. Thus the global phase portrait is shown in Figure 12.

In the case (I-5) one stable separatrix of the saddle P_- comes from the unstable node q_- and the second stable separatrix of P_- comes from the unstable node P_+. Two unstable separatrices of P_- goes to the stable node q_+. By the Poincáre-Bendixson theorem and by the type of stability of the equilibria we see the remaining orbits of the phase portrait where they start and where they end. Thus the global phase portrait is given in Figure 13.

In the case (I-6), one stable separatrix of the saddle P_- comes from the unstable node q_- and the second stable separatrix of P_- comes from the unstable node P_+. One unstable separatrix of P_- goes to the stable node q_+ and the second unstable separatrix of P_- goes to the semi-hyperbolic saddle-node p. An unstable separatrix of P_+ goes to p. We see the remaining orbits of the phase portrait by the Poincáre-Bendixson theorem and by the type of stability of the equilibria. Thus the global phase portrait is shown in Figure 14.

In the case (I-7) one stable separatrix of the saddle P_- comes from the unstable node q_- and the second stable separatrix of P_- comes from the unstable node P_+. One unstable separatrix of P_- goes to the stable node q_+ and the second unstable separatrix of P_- goes to the stable node p_+. An unstable separatrix of P_+ goes to the saddle p_-. By the Poincáre-Bendixson theorem and by the type of stability of the equilibria we get the remaining orbits of the phase portrait. Thus the global phase portrait is given in Figure 15.

3.2. **Phase portraits in the Poincaré disc of system (II).** By $(x, y, t) \to (-x, y, t)$, the system (II) becomes

$$S_+: \quad \dot{x} = \tilde{b}x + y, \qquad \dot{y} = -x + 1, \qquad \text{if } x \geq 0, \text{ and}$$

$$S_-: \quad \dot{x} = \tilde{a}x + y, \qquad \dot{y} = x + 1, \qquad \text{if } x \leq 0.$$

This is similar to system (I) by exchanging the position of $\tilde{a}$ and $\tilde{b}$. So we obtain the phase portraits in the Poincaré disc for system (II) by reversing the half plane $x \geq 0$ and $x \leq 0$ for system (I).

3.3. **Phase portraits in the Poincaré disc of system (III).**

3.3.1. *The finite equilibria.* Note that the differential system S_+ (respectively S_-) has the equilibrium $P_+ = (0,0)$ (respectively $P_- = (0,0)$). Namely $P_- = P_+ =: P$. Then the equilibrium P is real for both systems S_+ and S_-.

The eigenvalues of the equilibrium P_+ are $\lambda_- := (\hat{a} - \sqrt{\hat{a}^2 - 4})/2$ and $\lambda_+ := (\hat{a} + \sqrt{\hat{a}^2 - 4})/2$. So if $\hat{a} \leq -2$ (respectively $\hat{a} \geq 2$) then $\lambda_- < \lambda_+ < 0$ (respectively $\lambda_+ > \lambda_- > 0$), implying that P_+ is a stable (respectively an unstable) node. If $-2 < \hat{a} < 0$ (respectively $0 < \hat{a} < 2$) then $\lambda_\pm$ are a pair of imaginary eigenvalues with negative (respectively positive) real part, implying that P_+ is a stable (respectively an unstable) focus. If $\hat{a} = 0$ then $\lambda_\pm$ are a pair of purely imaginary eigenvalues, implying that P_+ is a center.

The eigenvalues of the equilibrium P_- are $\mu_- := (\hat{b} - \sqrt{\hat{b}^2 + 4})/2$ and $\mu_+ := (\hat{b} + \sqrt{\hat{b}^2 + 4})/2$. Clearly, $\mu_- < 0 < \mu_+$, implying that P_- is a saddle.

3.3.2. *The infinite equilibria.* We write the differential system S_+ in the local charts U_1 and U_2. Then in the local chart U_1 system S_+ writes

$$\dot{u} = 1 - \hat{a}u + u^2, \quad \dot{v} = -\hat{a}v + uv; \tag{16}$$

and in the local chart U_2 becomes

$$\dot{u} = -1 + \hat{a}u - u^2, \quad \dot{v} = -uv. \tag{17}$$

We separate the study of the infinite equilibria of system S_+ in three cases.

Case (III1$_+$): $\hat{a} > 2$ or $\hat{a} < -2$. Then there are only two infinite equilibria of system S_+ in the local chart U_1, namely $p_\pm = \big((\hat{a} \pm \sqrt{\hat{a}^2 - 4})/2, 0\big)$ and the origin of the local chart U_2 is not an infinite equilibrium.

The eigenvalues of the equilibrium p_+ are $\sqrt{\hat{a}^2 - 4}$ and $\lambda_p = -(\hat{a} - \sqrt{\hat{a}^2 - 4})/2$. If $\hat{a} > 2$ then $\lambda_p < 0$, implying that p_+ is a saddle, and if $\hat{a} < -2$ then $\lambda_p > 0$, implying that p_+ is an unstable node.

The eigenvalues of the equilibrium p_- are $-\sqrt{\hat{a}^2 - 4}$ and $\mu_p = -(\hat{a} + \sqrt{\hat{a}^2 - 4})/2$. If $\hat{a} > 2$ then $\mu_p < 0$, implying that p_- is a stable node, and if $\hat{a} < -2$ then $\mu_p > 0$, implying that p_- is a saddle.

Case (III2$_+$): $\hat{a} = -2$ and $\hat{a} = 2$. Then there is only one infinite equilibrium of system S_+ in the local chart U_1, namely $p = (\hat{a}/2, 0)$, and the origin O of the local chart U_2 is not an infinite equilibrium. The eigenvalues of the equilibrium p are 0 and $-\hat{a}/2 \neq 0$. Therefore by [3, Theorem 2.19] the infinite equilibrium p is a semi-hyperbolic saddle-node.

Case (III3$_+$): $-2 < \hat{a} < 2$. Then system S_+ has no infinite equilibria in the local chart U_1 and at the origin of the local chart U_2.

Again we write the differential system S_- in the local charts V_1 and U_2. Then in the local chart V_1 system S_- writes

$$\dot{u} = -1 - \hat{b}u + u^2, \quad \dot{v} = -\hat{b}v + uv; \tag{18}$$

and in the local chart U_2 becomes

$$\dot{u} = -1 + \hat{b}u + u^2, \quad \dot{v} = uv. \tag{19}$$

As we did for the system S_+, there are only two infinite equilibria of system S_- in the local chart V_1, namely $q_\pm = \left((\hat{b} \pm \sqrt{\hat{b}^2+4})/2, 0\right)$ and the origin of the local chart U_2 is not an infinite equilibrium.

The eigenvalues of the equilibrium q_+ are $\sqrt{\hat{b}^2+4}$ and $\lambda_q = -(\hat{b} - \sqrt{\hat{b}^2+4})/2$. Clearly, $\lambda_q > 0$, implying that q_+ is an unstable node. The eigenvalues of the equilibrium q_- are $-\sqrt{\tilde{b}^2+4}$ and $\mu_q = -(\tilde{b} + \sqrt{\tilde{b}^2+4})/2$. And therefore q_- is a stable node since $\mu_q < 0$.

In summary from the above discussion, we obtain the results of Table 3.

System	Conditions	Finite Equilibria	Infinite Equilibria
(III)	(III-1): $\hat{a} < -2$	P(stable node)	p_+(unstable node), p_-(saddle)
		P(saddle)	q_+(unstable node) q_-(stable node)
	(III-2): $\hat{a} = -2$	P(stable node)	p(semi-hyperbolic saddle-node),
		P(saddle)	q_+(unstable node) q_-(stable node)
	(III-3): $-2 < \hat{a} < 0$	P(stable focus)	
		P(saddle)	q_+(unstable node) q_-(stable node)
	(III-4): $\hat{a} = 0$	P(center)	
		P(saddle)	q_+(unstable node) q_-(stable node)
	(III-5): $0 < \hat{a} < 2$	P(unstable focus)	
		P(saddle)	q_+(unstable node) q_-(stable node)
	(III-6): $\hat{a} = 2$	P(unstable node)	p(semi-hyperbolic saddle-node),
		P(saddle)	q_+(unstable node) q_-(stable node)
	(III-7): $\hat{a} > 2$	P(unstable node)	p_+(saddle), p_-(stable node)
		P(saddle)	q_+(unstable node) q_-(stable node)

TABLE 3. The local phase portraits at the finite and infinite equilibria of the piecewise differential system (III).

3.3.3. *The global phase portraits in the Poincaré disc.* Similar to system (I), by (16)-(19) we see that the right hand sides of the equation $\dot{v}$ both have a common factor v, implying that the infinity is formed by orbits. Further check $\dot{x} = -y$ and $\dot{y} = 0$ on the y-axis. Then initiating at points lying on the positive y-axis, all orbits go into the half plane $x \leq 0$ while initiating at points lying in the negative y-axis, all orbits go into the half plane $x \geq 0$. On the other hand for system S_- there are the horizontal isocline $\mathcal{H} : x = 0$ and the vertical isocline $\mathcal{V} : y = \hat{b}x$. Also for system (16) there are two invariant lines $u = (\hat{a} \pm \sqrt{\hat{a}^2 - 4})/2$ and for system (18) there are two invariant lines $u = (\hat{b} \pm \sqrt{\hat{b}^2 + 4})/2$. According to Table 3, we below discuss the global phase portraits in the following several cases.

In the case (III-1) one stable separatrix of the stable node P in the half plane $x \geq 0$ comes from the unstable node p_+ lying on the line $y = ((\hat{a} + \sqrt{\hat{a}^2 - 4})/2)x$ and the second stable separatrix of the stable node P in the half plane $x \geq 0$ comes from the saddle p_- lying on the line $y = ((\hat{a} - \sqrt{\hat{a}^2 - 4})/2)x$. One stable separatrix of the saddle P in the half plane $x \leq 0$ comes from the unstable node q_+ lying on the line $y = ((\hat{b} + \sqrt{\hat{b}^2 + 4})/2)x$ and one unstable separatrix of P goes to the stable node q_- lying on the line $y = ((\hat{b} - \sqrt{\hat{b}^2 + 4})/2)x$. The remaining orbits of the phase portrait are determined where they start and where they end by the type of stability of the equilibria and by the Poincáre-Bendixson theorem. Thus the global phase portrait is shown in Figure 16.

Note that for the remain cases (III-2)-(III-7) the phase portrait is the same as the case (III-1) in the half plane $x \leq 0$. For the half plane $x \geq 0$ the phase portrait is studied in what follows.

In the case (III-2) one stable separatrix of the stable node P in the half plane $x \geq 0$ comes from the semi-hyperbolic saddle-node p lying on the line $y = (\hat{a}/2)x$. The remaining orbits of the phase portrait are determined by the type of stability of the equilibria and by the Poincáre-Bendixson theorem. Thus the global phase portrait is shown in Figure 17.

In cases (III-3)-(III-5) there is no separatrix in the half plane $x \geq 0$. The remaining orbits of the phase portrait are determined by the type of stability of the equilibria and by the Poincáre-Bendixson theorem. Thus the global phase portraits of these three cases are given in Figures 18.

In the case (III-6) an unstable separatrix of the unstable node P in the half plane $x \geq 0$ goes to the semi-hyperbolic saddle-node p lying on the line $y = \hat{a}/2x$. We get the remaining orbits of the phase portrait by the type of stability of the equilibria and by the Poincáre-Bendixson theorem. Thus the global phase portrait is shown in Figure 19.

In the case (III-7) one unstable separatrix of the unstable node P in the half plane $x \geq 0$ goes to the saddle p_+ lying on the line $y = ((\hat{a} + \sqrt{\hat{a}^2 - 4})/2)x$ and the second unstable separatrix of P in the half plane $x \geq 0$ goes to the stable node p_- lying on the line $y = ((\hat{a} - \sqrt{\hat{a}^2 - 4})/2)x$. We get the remaining orbits of the phase portrait by the type of stability of the equilibria and by the Poincáre-Bendixson theorem. Thus the global phase portrait is shown in Figure 20.

3.4. **Phase portraits in the Poincaré disc of system (IV).** Note that by exchanging the position of $\hat{a}$ and $\hat{b}$ then S_+ of system (III) is the same that S_- of system (IV), while S_- of system (III) is the same that S_+ of system (IV). So we obtain the phase portraits in the Poincaré disc for system (IV) by exchanging the half planes $x \geq 0$ and $x \leq 0$ of system (III).

3.5. **Phase portraits in the Poincaré disc of system (V).**

3.5.1. *The finite and infinite equilibria.* Note that the differential system S_+ has the equilibrium $P_+ = (-1, -a)$, while the differential system S_- has the equilibrium $P_- = (1, b)$. Then the equilibrium P_+ (respectively P_-) is virtual for the differential systems S_+ (respectively S_-).

Doing the change $(x, y, t) \to (-x, y, t)$, the system (V) becomes

$$S_+ : \quad \dot{x} = \tilde{b}x + y, \qquad \dot{y} = x + 1, \qquad \text{if } x \geq 0, \text{ and}$$

$$S_- : \quad \dot{x} = \tilde{a}x + y, \qquad \dot{y} = -x + 1, \qquad \text{if } x \leq 0, \text{ and.}$$

The system S_+ is the same that S_- of system (I) while the system S_- is the same that S_+ of system (I). So from the results of system (I) for the finite and infinite equilibria of system (V) we get the Table 4.

System	Conditions	Finite Equilibria	Infinite Equilibria
(V)	(V-1): $\tilde{a} < -2$	P_+(stable node)	p_+(unstable node), p_-(saddle)
		P_-(saddle)	q_+(unstable node) q_-(stable node)
	(V-2): $\tilde{a} = -2$	P_+(stable node)	p(semi-hyperbolic saddle-node)
		P_-(saddle)	q_+(unstable node) q_-(stable node)
	(V-3): $-2 < \tilde{a} < 0$	P_+(stable focus)	
		P_-(saddle)	q_+(unstable node) q_-(stable node)
	(V-4): $\tilde{a} = 0$	P_+(center)	
		P_-(saddle)	q_+(unstable node) q_-(stable node)
	(V-5): $0 < \tilde{a} < 2$	P_+(unstable focus)	
		P_-(saddle)	q_+(unstable node) q_-(stable node)
	(V-6): $\tilde{a} = 2$	P_+(unstable node)	p(semi-hyperbolic saddle-node)
		P_-(saddle)	q_+(unstable node) q_-(stable node)
	(V-7): $\tilde{a} > 2$	P_+(unstable node)	p_+(saddle) p_-(stable node)
		P_-(saddle)	q_+(unstable node) q_-(stable node)

TABLE 4. The local phase portraits at the finite and infinite equilibria of the piecewise differential system (V).

3.5.2. *The global phase portraits in the Poincaré disc.* Similar to system (I), we check $\dot{x} = -y$ and $\dot{y} = 1$ on the y-axis. Then initiating at points lying on the positive y-axis all orbits go into the half plane $x \leq 0$, while initiating at points lying in the negative y-axis all orbits go into the half plane $x \geq 0$. On the other hand the infinity is formed by orbits. According to Table 4, we below discuss the global phase portraits in the following several cases.

In the case (V-1) a separatrix comes from the saddle p_- going to the stable node q_-. The remaining orbits of the phase portrait are determined where they start and where they end by the type of stability of the equilibria and by the Poincáre-Bendixson theorem. Thus the global phase portrait is given in Figure 21.

In the case (V-2) a separatrix comes from the semi-hyperbolic saddle-node p going to the stable node q_-. By the type of stability of the equilibria and by the Poincáre-Bendixson theorem we get the remaining orbits of the phase portrait. Thus the global phase portrait is given in Figure 22.

In the case (V-3)-(V-5), there is no separatrix in the phase portrait. All orbits leave q_+ for q_-. Thus the global phase portrait is shown in Figure 23.

In the case (V-6) a separatrix comes from the unstable node q_+ going to the semi-hyperbolic saddle-node p. The remaining orbits of the phase portrait are determined by the type of stability of the equilibria and by the Poincáre-Bendixson theorem. Thus the global phase portrait is shown in Figure 24.

In the case (V-7) a separatrix comes from the unstable node q_+ going to the saddle p_+. Similarly we get the remaining orbits of the phase portrait. Thus the global phase portrait is shown in Figure 25.

3.6. **Phase portraits in the Poincaré disc of system (VI).** Note that by exchanging the position of $\hat{a}$ and $\hat{b}$ then S_+ of system (VI) is the same that S_- of system (I), while S_- of system (VI) is the same that S_+ of system (I). So we obtain the phase portraits in the Poincaré disc for system (VI) by exchanging the half planes $x \geq 0$ and $x \leq 0$ of system (I).

System	Conditions	Finite Equilibria	Infinite Equilibria
(VII)	(VII-1): $\check{b} < -1$	P_+(saddle)	p(stable node), O(unstable node)
		P_-(stable node)	q(saddle) O(unstable node)
	(VII-2): $\check{b} = -1, \check{\check{a}} < 0$	P_+(saddle)	p(stable node) O(unstable node)
		P_-(stable node)	O(semi-hyperbolic saddle-node)
	(VII-3): $\check{b} = -1, \check{\check{a}} = 0$	P_+(saddle)	p(stable node) O(unstable node)
		P_-(stable node)	u-axis(starts an orbit) O(starts an orbit)
	(VII-4): $\check{b} = -1, \check{\check{a}} > 0$	P_+(saddle)	p(stable node) O(unstable node)
		P_-(stable node)	O(semi-hyperbolic saddle-node)
	(VII-5): $-1 < \check{b} < 0$	P_+(saddle)	p(stable node) O(unstable node)
		P_-(stable node)	q(unstable node) O(saddle)
	(VII-6): $0 < \check{b} < 1$	P_+(unstable node)	p(stable node) O(saddle)
		P_-(saddle)	q(unstable node) O(stable node)
	(VII-7): $\check{b} = 1, \check{\check{a}} < 0$	P_+(unstable node)	O(semi-hyperbolic saddle-node)
		P_-(saddle)	q(unstable node) O(stable node)
	(VII-8): $\check{b} = 1, \check{\check{a}} = 0$	P_+(unstable node)	u-axis(ends an orbit) O(ends an orbit)
		P_-(saddle)	q(unstable node) O(stable node)
	(VII-9): $\check{b} = 1, \check{\check{a}} > 0$	P_+(unstable node)	O(semi-hyperbolic saddle-node)
		P_-(saddle)	q(unstable node) O(stable node)
	(VII-10): (VII-10): $\check{b} = 1, \check{b} > 1$	P_+(unstable node)	p(saddle) O(stable node)
		P_-(saddle)	q(unstable node) O(stable node)

TABLE 5. The local phase portraits at the finite and infinite equilibria of the piecewise differential system (VII).

3.7. **Phase portraits in the Poincaré disc of system (VII).**

3.7.1. *The finite equilibria.* Note that $\check{b} = \beta/|a| \neq 0$, otherwise $a\beta - \alpha b = 0$ because $b = 0$ in the case. Then the differential system S_+ has the equilibrium $P_+ = \big(1, -\check{a}/\check{b}\big)$. While the differential system S_- has the equilibrium $P_- = \big(-1, -\check{a}/\check{b}\big)$. Moreover the equilibrium P_+ (respectively P_-) is real for the differential system S_+ (respectively S_-).

The eigenvalues of the equilibrium P_+ are 1 and $\check{b}$. So if $\check{b} > 0$ (respectively $\check{b} < 0$) then P_+ is an unstable node (respectively a saddle). The eigenvalues of the equilibrium P_- are -1 and $\check{b}$. Then P_- is a saddle if $\check{b} > 0$ and a stable node if $\check{b} < 0$.

3.7.2. *The infinite equilibria.* We write the differential system S_+ in the local charts U_1 and becomes

$$\dot{u} = \check{a} + (\check{b} - 1)u + uv, \quad \dot{v} = -v + v^2; \tag{20}$$

and in the local chart U_2 becomes

$$\dot{u} = (1 - \check{b})u - v - \check{a}u^2, \quad \dot{v} = -\check{b}v - \check{a}uv. \tag{21}$$

We separate the study of the infinite equilibria of system S_+ in two cases.

Case (VII1$_+$): $\check{b} \neq 1$. Then there is only one infinite equilibrium of system S_+ in the local chart U_1, namely $p = \big(-\check{a}/(\check{b} - 1), 0\big)$ and the origin O of the local chart U_2 is an infinite equilibrium. The eigenvalues of the equilibrium p are -1 and $\check{b} - 1$. Thus p is a stable node if $\check{b} < 1$ and a saddle if $\check{b} > 1$. The eigenvalues of the equilibrium O are $1 - \check{b}$ and $-b$. Then O is an unstable node if $\check{b} < 0$, a semi-hyperbolic saddle-node if $\check{b} = 0$, a saddle if $0 < \check{b} < 1$ and a stable node $\check{b} > 1$.

Case (VII2$_+$): $\check{b} = 1$. We consider two subcases: $\check{a} \neq 0$ and $\check{a} = 0$. In the first subcase there is no infinite equilibrium in the local chart U_1 but the origin O of the local chart U_2 is an infinite equilibrium. Moreover the eigenvalues of O are 0 and -1, implying that it is a semi-hyperbolic saddle-node. In the second subcase all points on the u-axis are infinite equilibria in the local chart V_1 for system S_+. Since the eigenvalues at each one of these equilibria are 0 and $-1 \neq 0$, by the normally hyperbolic equilibria theorem (see [6]) it follows that at each one of these equilibria ends an orbit. The origin of the local chart U_2 is also an equilibrium inside the continuum of equilibria at infinity with eigenvalues 0 and -1, so the same conclusion for it.

Again we write the differential system S_- in the local charts V_1 and U_2. Then in the local chart V_1 system S_- writes

$$\dot{u} = -\check{a} + (\check{b} + 1)u + uv, \quad \dot{v} = v + v^2; \tag{22}$$

and in the local chart U_2 becomes

$$\dot{u} = -(1 + \check{b})u - v + \check{a}u^2, \quad \dot{v} = -\check{b}v + \check{a}uv. \tag{23}$$

As we did for the system S_+, We separate the study of the infinite equilibria of system S_- in two cases.

Case (VII1$_-$): $\check{b} \neq -1$. Then there is only one infinite equilibrium of system S_- in the local chart V_1, namely $q = \big(\check{a}/(\check{b} + 1), 0\big)$ and the origin O of the local chart U_2 is an infinite equilibrium. The eigenvalues of the equilibrium q are 1 and $\check{b} + 1$. Then q is a saddle if $\check{b} < -1$ and an unstable node if $\check{b} > -1$. The eigenvalues of the equilibrium O are $-1 - \check{b}$ and $-b$. Then O is an unstable node if $\check{b} < -1$, a saddle if $-1 < \check{b} < 0$, a semi-hyperbolic saddle-node if $\check{b} = 0$ and a stable node $\check{b} > 0$.

Case (VII2$_-$): $\check{b} = -1$. Again we consider two subcases: $\check{a} \neq 0$ and $\check{a} = 0$. In the first subcase there is no infinite equilibrium in the local chart U_1 but the origin O of the local chart U_2 is an infinite equilibrium. Moreover the eigenvalues of O are 0 and 1, implying that it is a semi-hyperbolic saddle-node. In the second subcase all points on the u-axis are infinite equilibria in the local chart V_1 for system S_-. Since the eigenvalues at each one of these equilibria are

0 and $1 \neq 0$, by the normally hyperbolic equilibria theorem each one of these equilibria starts an orbit. At the origin of the local chart U_2 we also have a semi-hyperbolic saddle-node.

In summary from the above discussion, we obtain the results of Table 5.

3.7.3. *The global phase portraits in the Poincaré disc.* First we see $\dot{x} = -1$ on the y-axis. Then initiating at points lying on the positive y-axis all orbits go into the half plane $x < 0$. On the other hand the infinity as always is formed by orbits because the equation $\dot{v}$ of equations (20)-(23) has a common factor v. According to Table 5, we divide the study of the global phase portraits in the following cases.

In the case (VII-1) one stable separatrix of the saddle P_+ comes from the unstable node O in the positive y-direction and the second stable separatrix of P_+ comes from the unstable node O in the negative y-direction. One unstable separatrix of P_+ goes to the stable node p and the second unstable separatrix of P_+ goes to the stable node P_-. A stable separatrix of P_- comes from the saddle q. The remaining orbits of the phase portrait are determined where they start and they end by the type of stability of the equilibria and by the Poincáre-Bendixson theorem. Thus the global phase portrait is shown in Figure 26.

In the case (VII-2) one stable separatrix of the saddle P_+ comes from the semi-hyperbolic saddle-node O in the positive y-direction and the second stable separatrix of P_+ comes from the unstable node O in the negative y-direction. One unstable separatrix of P_+ goes to the stable node p and the second unstable separatrix of P_+ goes to the stable node P_-. The remaining orbits of the phase portrait are determined by the type of stability of the equilibria and by the Poincáre-Bendixson theorem. Thus the global phase portrait is shown in Figure 27.

In the case (VII-3) one stable separatrix of the saddle P_+ comes from the unstable node O in the positive y-direction and the second stable separatrix of P_+ comes from the equilibrium O in the negative y-direction. One unstable separatrix of P_+ goes to the stable node p and the second unstable separatrix of P_+ goes to the stable node P_-. The remaining orbits of the phase portrait are determined by the type of stability of the equilibria and by the Poincáre-Bendixson theorem. Thus the global phase portrait is shown in Figure 28.

In the case (VII-4) one stable separatrix of the saddle P_+ comes from the unstable node O in the positive y-direction and the second stable separatrix of P_+ comes from the semi-hyperbolic saddle node O in the negative y-direction. One unstable separatrix of P_+ goes to the stable node p and the second unstable separatrix of P_+ goes to the stable node P_-. A stable separatrix of P_- comes from the unstable node O in the positive y-direction. The remaining orbits of the phase portrait are determined by the type of stability of the equilibria and by the Poincáre-Bendixson theorem. Thus the global phase portrait is shown in Figure 29.

In the case (VII-5) one stable separatrix of the saddle P_+ comes from the unstable node O in the positive y-direction and the second stable separatrix of P_+ comes from the saddle O in the negative y-direction. One unstable separatrix of P_+ goes to the stable node p and the second unstable separatrix of P_+ goes to the stable node P_-. One stable separatrix of the saddle P_- comes from the unstable node O in the positive y-direction and the second stable separatrix of P_- comes from the saddle O in the negative y-direction. By the type of stability of the equilibria and by the Poincáre-Bendixson theorem we get the remaining orbits of the phase portrait. Thus the global phase portrait is shown in Figure 30.

In the case (VII-6) one stable separatrix of the saddle P_- comes from the unstable node q and the second stable separatrix of P_- comes from the unstable node P_+. One unstable separatrix of P_- comes from the saddle O in the positive y-direction and the second stable separatrix of P_- comes from the stable node O in the negative y-direction. One unstable separatrix of the unstable node P_+ goes to the saddle O in the positive y-direction and the second unstable separatrix of P_+ goes to the stable node O in the negative y-direction. Similarly we get the remaining orbits of the phase portrait by the type of stability of the equilibria and by the Poincáre-Bendixson theorem. Thus the global phase portrait is shown in Figure 31.

In the case (VII-7) one stable separatrix of the saddle P_- comes from the unstable node q and the second stable separatrix of P_- comes from the unstable node P_+. One unstable separatrix of P_- goes to the semi-hyperbolic saddle-node O in the positive y-direction and the second unstable separatrix of P_- goes to the stable node O in the negative y-direction. An unstable separatrix of P_+ goes to the semi-hyperbolic saddle-node O in the positive y-direction. The remaining orbits of the phase portrait are determined by the type of stability of the equilibria and by the Poincáre-Bendixson theorem. Thus the global phase portrait is shown in Figure 32.

In the case (VII-8) one stable separatrix of the saddle P_- comes from the unstable node q and the second stable separatrix of P_- comes from the unstable node P_+. One unstable separatrix of P_- goes to the equilibrium O in the positive y-direction and the second unstable separatrix of P_- goes to the stable node O in the negative y-direction. The remaining orbits of the phase portrait are determined by the type of stability of the equilibria and by the Poincáre-Bendixson theorem. Thus the global phase portrait is shown in Figure 33.

In the case (VII-9) one stable separatrix of the saddle P_- comes from the unstable node q and the second stable separatrix of P_- comes from the unstable node P_+. One unstable separatrix of P_- goes to the semi-hyperbolic saddle-node O in the positive y-direction and the second unstable separatrix of P_- goes to the stable node O in the negative y-direction. An unstable separatrix of P_+ goes to the stable node O in the negative y-direction. Similar to the above, we get the remaining orbits of phase portrait. Thus the global phase portrait is shown in Figure 34.

In the case (VII-10) one stable separatrix of the saddle P_- comes from the unstable node q and the second stable separatrix of P_- comes from the unstable node P_+. One unstable separatrix of P_- goes to the stable node O in the positive y-direction and the second unstable separatrix of P_- goes to the stable node O in the positive y-direction. An unstable separatrix of P_+ goes to the saddle p. Similarly we get the remaining orbits of the phase portrait by the type of stability of the equilibria and by the Poincáre-Bendixson theorem. Thus the global phase portrait is shown in Figure 35.

3.8. **Phase portraits in the Poincaré disc of system (VIII).**

3.8.1. *The finite and infinite equilibria.* Note that S_+ of system (VIII) is the same that S_- of system (VII) if we regard $\check{\check{a}}$ as $-\check{a}$. While S_- of system (VIII) is also the same that S_+ of system (VII). So from the results of system (VII) for the finite and infinite equilibria of system (VIII) we get the Table 6. Note that the equilibria $P_+ = \big(-1, \check{a}/\check{b}\big)$ and $P_- = \big(1, \check{a}/\check{b}\big)$ are virtual.

3.8.2. *The global phase portraits in the Poincaré disc.* According to Table 6, we below discuss the global phase portraits in the following several cases.

In the case (VIII-1) a separatrix comes from the saddle p, then goes to the stable node q. The remaining orbits of the phase portrait are determined where they start and they end by the type of stability of the equilibria and by the Poincáre-Bendixson theorem. Thus the global phase portrait is shown in Figure 36.

In the case (VIII-2) a separatrix comes from the unstable node O in the negative y-direction, then goes to the stable node q. The remaining orbits of the phase portrait are determined by the type of stability of the equilibria and by the Poincáre-Bendixson theorem. Thus the global phase portrait is shown in Figure 37.

In the case (VIII-3) all orbits start from the infinity in the half plane $x \geq 0$, then go to the stable node q. Thus the global phase portrait is shown in Figure 38.

In the case (VIII-4) a separatrix starts from the semi-hyperbolic saddle-node O in the positive y-direction, then goes to the stable node q. We similarly get the remaining orbits of the phase portrait by the type of stability of the equilibria and by the Poincáre-Bendixson theorem. Thus the global phase portrait is shown in Figure 39.

In the case (VIII-5) one separatrix starts from the saddle O in the positive y-direction, then goes to the stable node q. The second separatrix starts from the unstable node O in the negative y-direction, then goes to q. The remaining orbits in the phase portrait are determined by the type of stability of the equilibria and by the Poincáre-Bendixson theorem. Thus the global phase portrait is shown in Figure 40.

In the case (VIII-6) one separatrix starts from the saddle O in the positive y-direction, then goes to the stable node q. The second separatrix starts from the unstable node O in the negative y-direction, then goes to q. The remaining orbits in the phase portrait are determined by the type of stability of the equilibria and by the Poincáre-Bendixson theorem. Thus the global phase portrait is shown in Figure 41.

In the case (VIII-7) a separatrix comes from the unstable node p, then goes to the stable node O in the positive y-direction. We get the remaining orbits by the type of stability of the equilibria and by the Poincáre-Bendixson theorem. Thus the global phase portrait is shown in Figure 42.

In the case (VIII-8) all orbits come from the unstable node p, then go to the infinity of the half plane $x \leq 0$. Thus the global phase portrait is shown in Figure 43.

In the case (VIII-9) a separatrix comes from the unstable node p, then goes to the semi-hyperbolic saddle node O in the negative y-direction. We obtain the remaining orbits by the type of stability of the equilibria and by the Poincáre-Bendixson theorem. Thus the global phase portrait is shown in Figure 44.

In the case (VIII-10) a separatrix comes from the unstable node p, then goes to the saddle q. We similarly get the remaining orbits by the type of stability of the equilibria and by the Poincáre-Bendixson theorem. Thus the global phase portrait is shown in Figure 45.

3.9. **Phase portraits in the Poincaré disc of system (IX).**

3.9.1. *The finite equilibria.* Note that the differential system S_+ (respectively S_-) has the equilibrium $P_+ = (0,0)$ (respectively $P_- = (0,0)$). Namely $P_- = P_+ =: P$. Then the equilibrium P is real for both systems S_+ and S_-.

The eigenvalues of the equilibrium P_+ are 1 and $\check{b}$. So if $\check{b} > 0$ (respectively $\check{b} < 0$) then P_+ is an unstable node (respectively a saddle). The eigenvalues of the equilibrium P_- are -1 and $\check{b}$. Then P_- is a saddle if $\check{b} > 0$ and a stable node if $\check{b} < 0$.

3.9.2. *The infinite equilibria.* We write the differential system S_+ in the local charts U_1 and becomes

$$\dot{u} = \check{a} + (\check{b} - 1)u, \quad \dot{v} = -v;$$

and in the local chart U_2 becomes

$$\dot{u} = (1 - \check{b})u - \check{a}u^2, \quad \dot{v} = -\check{b}v - \check{a}uv.$$

We separate the study of the infinite equilibria of system S_+ in two cases.

Case (IX1_+): $\check{b} \neq 1$. Then there is only one infinite equilibrium of system S_+ in the local chart U_1, namely $p = \big(-\check{a}/(\check{b} - 1), 0\big)$ and the origin O of the local chart U_2 is an infinite equilibrium. The eigenvalues of the equilibrium p are -1 and $\check{b} - 1$. Thus p is a stable node if $\check{b} < 1$ and a saddle if $\check{b} > 1$. The eigenvalues of the equilibrium O are $1 - \check{b}$ and $-b$. Then O is an unstable node if $\check{b} < 0$, a semi-hyperbolic saddle-node if $\check{b} = 0$, a saddle if $0 < \check{b} < 1$ and a stable node $\check{b} > 1$.

Case (IX2_+): $\check{b} = 1$. We consider two subcases: $\check{a} \neq 0$ and $\check{a} = 0$. In the first subcase there is no infinite equilibrium in the local chart U_1 but the origin O of the local chart U_2 is an infinite equilibrium. Moreover the eigenvalues of O are 0 and -1, implying that it is a semi-hyperbolic saddle-node. In the second subcase all points on the u-axis are infinite equilibria in the local chart V_1 for system S_+. Since the eigenvalues at each one of these equilibria are 0 and $-1 \neq 0$,

System	Conditions	Finite Equilibria	Infinite Equilibria
(VIII)	(VIII-1): $\check{b} < -1$	P_+(stable node)	p(saddle) O(unstable node)
		P_-(saddle)	q(stable node) O(unstable node)
	(VIII-2): $\check{b} = -1, \check{\check{a}} < 0$	P_+(stable node)	O(semi-hyperbolic saddle-node)
		P_-(saddle)	q(stable node) O(unstable node)
	(VIII-3): $\check{b} = -1, \check{\check{a}} = 0$	P_+(stable node)	u-axis(starts an orbit) O(starts an orbit)
		P_-(saddle)	q(stable node) O(unstable node)
	(VIII-4):$\check{b} = -1, \check{\check{a}} > 0$	P_+(stable node)	O(semi-hyperbolic saddle-node)
		P_-(saddle)	q(stable node) O(unstable node)
	(VIII-5): $-1 < \check{b} < 0$	P_+(stable node)	p(unstable node) O(saddle)
		P_-(saddle)	q(stable node) O(unstable node)
	(VIII-6): $0 < \check{b} < 1$	P_+(saddle)	p(unstable node) O(stable node)
		P_-(unstable node)	q(stable node) O(saddle)
	(VIII-7): $\check{b} = 1, \check{\check{a}} < 0$	P_+(saddle)	p(unstable node) O(stable node)
		P_-(unstable node)	O(semi-hyperbolic saddle-node)
	(VIII-8): $\check{b} = 1, \check{\check{a}} = 0$	P_+(saddle)	p(unstable node) O(stable node)
		P_-(unstable node)	u-axis(ends an orbit) O(ends an orbit)
	(VIII-9): $\check{b} = 1, \check{\check{a}} > 0$	P_+(saddle)	p(unstable node) O(stable node)
		P_-(unstable node)	O(semi-hyperbolic saddle-node)
	(VIII-10): $\check{b} > 1$	P_-(saddle)	p(unstable node) O(stable node)
		P_+(unstable node)	q(saddle) O(stable node)

Table 6. The local phase portraits at the finite and infinite equilibria of the piecewise differential system (VIII).

it follows that at each one of these equilibria ends an orbit. The origin of the local chart U_2 is also an equilibrium inside the continuum of equilibria at infinity with eigenvalues 0 and -1, so the same conclusion for it.

Again we write the differential system S_- in the local charts V_1 and U_2. Then in the local chart V_1 system S_- writes

$$\dot{u} = -\check{a} + (\check{b}+1)u, \quad \dot{v} = v;$$

and in the local chart U_2 becomes

$$\dot{u} = -(1+\check{b})u + \check{a}u^2, \quad \dot{v} = -\check{b}v + \check{a}uv.$$

As we did for the system S_+, We separate the study of the infinite equilibria of system S_- in two cases.

Case (IX1$_-$): $\check{b} \neq -1$. Then there is only one infinite equilibrium of system S_- in the local chart V_1, namely $q = \big(\check{a}/(\check{b}+1), 0\big)$ and the origin O of the local chart U_2 is an infinite equilibrium. The eigenvalues of the equilibrium q are 1 and $\check{b}+1$. Then q is a saddle if $\check{b} < -1$ and an unstable node if $\check{b} > -1$. The eigenvalues of the equilibrium O are $-1-\check{b}$ and $-b$. Then O is an unstable node if $\check{b} < -1$, a saddle if $-1 < \check{b} < 0$, a semi-hyperbolic saddle-node if $\check{b} = 0$ and a stable node $\check{b} > 0$.

Case (IX2$_-$): $\check{b} = -1$. Again we consider two subcases: $\check{a} \neq 0$ and $\check{a} = 0$. In the first subcase there is no infinite equilibrium in the local chart U_1 but the origin O of the local chart U_2 is an infinite equilibrium. Moreover the eigenvalues of O are 0 and 1, implying that it is a semi-hyperbolic saddle-node. In the second subcase all points on the u-axis are infinite equilibria in the local chart V_1 for system S_-. Since the eigenvalues at each one of these equilibria are 0 and $1 \neq 0$, each one of these equilibria starts an orbit. At the origin of the local chart U_2 we also have a semi-hyperbolic saddle-node.

In summary from the above discussion, we obtain the results of Table 7.

3.9.3. *The global phase portraits in the Poincaré disc.* Note that $\dot{x} = 0$ and $\dot{y} = \check{b}y$ when $x = 0$. This implies that the y-axis is invariant, i.e., the y-axis is formed by orbits. According to Table 7, we divide the study of the global phase portraits in the following cases.

In the case (IX-1) one stable separatrix of P comes from the unstable node O in the positive y-direction, the second stable separatrix of P comes from the unstable node O in the negative y-direction, and the third stable separatrix of P comes from the saddle q. An unstable separatrix of P goes to the stable node p. The remaining orbits of the phase portrait are determined where they start and they end by the type of stability of the equilibria and by the Poincáre-Bendixson theorem. Thus the global phase portrait is shown in Figure 46.

In the case (IX-2) one stable separatrix of P comes from the unstable node O in the positive y-direction and the second stable separatrix of P comes from the semi-hyperbolic saddle-node O in the negative y-direction. An unstable separatrix of P goes to the stable node p. The remaining orbits of the phase portrait are determined by the type of stability of the equilibria and by the Poincáre-Bendixson theorem. Thus the global phase portrait is shown in Figure 47.

In the case (IX-3) one stable separatrix of P comes from the unstable node O in the positive y-direction and the second stable separatrix of P comes from the degenerate equilibrium O in the negative y-direction. An unstable separatrix of P goes to the stable node p. On the other hand initiating at infinity in the half plane $x < 0$ all orbits go to P. The remaining orbits of the phase portrait are determined by the type of stability of the equilibria and by the Poincáre-Bendixson theorem. Thus the global phase portrait is shown in Figure 48.

In the case (IX-4) one stable separatrix of P comes from the unstable node O in the positive y-direction and the second stable separatrix of P comes from the semi-hyperbolic saddle-node O in the negative y-direction. An unstable separatrix of P goes to the stable node p. The remaining orbits of the phase portrait are determined by the type of stability of the equilibria and by the Poincáre-Bendixson theorem. Thus the global phase portrait is shown in Figure 49.

In the case (IX-5) one stable separatrix of P comes from the unstable node O in the positive y-direction and the second stable separatrix of P comes from the saddle O in the negative y-direction. An unstable separatrix of P goes to the stable node p. The remaining orbits of the phase portrait are determined by the type of stability of the equilibria and by the Poincáre-Bendixson theorem. Thus the global phase portrait is shown in Figure 50.

In the case (IX-6) one unstable separatrix of P goes to the saddle O in the positive y-direction and the second unstable separatrix of P goes to the stable node O in the negative y-direction. A stable separatrix of P comes from the unstable node q. The remaining orbits of the phase

System	Conditions	Finite Equilibria	Infinite Equilibria
(IX)	(IX-1): $\check{b} < -1$	P(saddle)	p(stable node), O(unstable node)
		P(stable node)	q(saddle) O(unstable node)
	(IX-2): $\check{b} = -1, \check{a} < 0$	P(saddle)	p(stable node) O(unstable node)
		P(stable node)	O(semi-hyperbolic saddle-node)
	(IX-3): $\check{b} = -1, \check{a} = 0$	P(saddle)	p(stable node) O(unstable node)
		P(stable node)	u-axis(starts an orbit) O(starts an orbit)
	(IX-4): $\check{b} = -1, \check{a} > 0$	P(saddle)	p(stable node) O(unstable node)
		P(stable node)	O(semi-hyperbolic saddle-node)
	(IX-5): $-1 < \check{b} < 0$	P(saddle)	p(stable node) O(unstable node)
		P(stable node)	q(unstable node) O(saddle)
	(IX-6): $0 < \check{b} < 1$	P(unstable node)	p(stable node) O(saddle)
		P(saddle)	q(unstable node) O(stable node)
	(IX-7): $\check{b} = 1, \check{a} < 0$	P(unstable node)	O(semi-hyperbolic saddle-node)
		P(saddle)	q(unstable node) O(stable node)
	(IX-8): $\check{b} = 1, \check{a} = 0$	P(unstable node)	u-axis(ends an orbit) O(ends an orbit)
		P(saddle)	q(unstable node) O(stable node)
	(IX-9): $\check{b} = 1, \check{a} > 0$	P(unstable node)	O(semi-hyperbolic saddle-node)
		P(saddle)	q(unstable node) O(stable node)
	(IX-10): $\check{b} > 1$	P(unstable node)	p(saddle) O(stable node)
		P(saddle)	q(unstable node) O(stable node)

TABLE 7. The local phase portraits at the finite and infinite equilibria of the piecewise differential system (IX).

portrait are determined by the type of stability of the equilibria and by the Poincáre-Bendixson theorem. Thus the global phase portrait is shown in Figure 51.

In the case (IX-7) one unstable separatrix of P goes to the semi-hyperbolic saddle-node O in the positive y-direction and the second unstable separatrix of P goes to the stable node O in the negative y-direction. A stable separatrix of P comes from the unstable node q. On the other hand by the type of stability of the equilibria and by the Poincáre-Bendixson theorem we get the remaining orbits of the phase portrait. Thus the global phase portrait is shown in Figure 52.

In the case (IX-8) one unstable separatrix of P goes to the degenerate equilibrium O in the positive y-direction and the second unstable separatrix of P goes to the stable node O in the negative y-direction. A stable separatrix of P comes from the unstable node q. On the other hand all orbits start from P going to the infinity in the half plane $x > 0$. By the type of stability of the equilibria and by the Poincáre-Bendixson theorem we get the remaining orbits of the phase portrait. Thus the global phase portrait is shown in Figure 53.

In the case (IX-9) a stable separatrix of P comes from the unstable node q. One unstable separatrix of P goes to the semi-hyperbolic saddle-node O in the positive y-direction. The second unstable separatrix of P goes to the stable node O in the negative y-direction. By the type of stability of the equilibria and by the Poincáre-Bendixson theorem we get the remaining orbits of the phase portrait. Thus the global phase portrait is shown in Figure 54.

In the case (IX-910) a stable separatrix of P comes from the unstable node q. One unstable separatrix of P goes to the stable node O in the positive y-direction, the second unstable separatrix of P goes to the stable node O in the negative y-direction, and the third unstable separatrix of P goes to the saddle p. We obtain the remaining orbits of the phase portraits by the type of stability of the equilibria and by the Poincáre-Bendixson theorem. Thus the global phase portrait is shown in Figure 55.

3.10. **Phase portraits in the Poincaré disc of system (X).** Note that S_+ of system (X) is the same that S_- of system (IX) if we regard $\breve{a}$ as $-\breve{a}$. While S_- of system (X) is also the same that S_+ of system (IX). Thus we obtain the result of Table 7 for finite and infinite equilibria. So we obtain the phase portraits in the Poincaré disc for system (X) by exchanging the half planes $x \geq 0$ and $x \leq 0$ of system (IX).

3.11. **Phase portraits in the Poincaré disc of system (XI).** By $(x, y, \breve{a}, \breve{b}, t) \to (x, y, -\breve{a}, -\breve{b}, -t)$, system (XI) is changed to system (VIII). Then we obtain the global phase portraits of system (XI) with parameters $(\breve{a}, \breve{b})$ by changing the direction of orbits for system (VIII) with parameters $(-\breve{a}, -\breve{b})$.

3.12. **Phase portraits in the Poincaré disc of system (XII).** By $(x, y, \breve{a}, \breve{b}, t) \to (x, y, -\breve{a}, -\breve{b}, -t)$, system (XII) is changed to system (VII). Then we obtain the global phase portraits of system (XII) with parameters $(\breve{a}, \breve{b})$ by changing the direction of orbits for system (VII) with parameters $(-\breve{a}, -\breve{b})$.

4. The distinct topologically equivalent phase portraits

In this section we summarize results on distinct topological equivalent phase portraits in Figures 7 and 55. By the separatrix configuration of the phase portrait in Theorem 2 we have the following 18 categories

1: Figures 7, 15, 26 and 35 are topologically equivalent;
2: Figures 8 and 27 are topologically equivalent;
3: Figures 9 and 13 are topologically equivalent;
4: Figures 10 and 11 are topologically equivalent;
5: Figure 12;
6: Figures 14, 29, 32 and 34 are topologically equivalent;
7: Figures 16, 20, 46 and 55 are topologically equivalent;
8: Figures 17, 19, 47, 49, 52 and 54 are topologically equivalent;
9: Figure 18;
10: Figures 21, 25, 36 and 45 are topologically equivalent;
11: Figures 22, 24, 37, 39, 42 and 44 are topologically equivalent;
12: Figure 23;
13: Figures 28 and 33 are topologically equivalent;
14: Figures 30 and 31 are topologically equivalent;
15: Figures 38 and 43 are topologically equivalent;

16: Figures 40 and 41 are topologically equivalent;
17: Figures 48 and 53 are topologically equivalent;
18: Figures 50 and 51 are topologically equivalent.

This completes the proof of Theorem 1.

Acknowledgements

The first author is partially supported by the China Scholarship Council (CSC) and by the national natural science foundation of China (NSFC) grants #11771307.

The second author is partially by Agencia Estatal de Investigación grant PID2019-104658GB-I00 (FEDER), the Agència de Gestió d'Ajuts Universitaris i de Recerca grant 2017SGR1617, and the H2020 European Research Council grant MSCA-RISE-2017-777911.

References

[1] A. Andronov, A. Vitt and S. Khaikin, *Theory of Oscillations*, Pergamon Press, Oxford, 1966.

[2] M. di Bernardo, C.J. Budd, A.R. Champneys, P. Kowalczyk, *Piecewise-Smooth Dynamical Systems: Theory and Applications*, Appl. Math. Sci. Series 163, Springer-Verlag, London, 2008.

[3] F. Dumortier, J. Llibre and J.C. Artés, *Qualitative Theory of Planar Differential Systems*, Springer Verlag, New York, 2006.

[4] E. Freire, E. Ponce, F. Rodrigo and F. Torres, *Bifurcation sets of continuous piecewise linear systems with two zones*, Int. J. Bifurcation and Chaos **8** (1998), 2073–2097.

[5] E. Freire, E. Ponce and F. Torres, *Canonical Discontinuous Planar Piecewise Linear Systems*, SIAM J. Appl. Dyn. Syst. **119** (2012), 181–211.

[6] M.W. Hirsch, C.C. Pugh and M. Shub, *Invariant manifolds*, Lecture Notes in Mathematics, Vol. **583**, Springer-Verlag, Berlin-New York, 1977.

[7] J. Llibre, M. Ordóñez and E. Ponce, *On the existence and uniqueness of limit cycles in a planar piecewise linear systems without symmetry*, Nonlinear Analysis Series B: Real World Applications **14** (2013), 2002–2012.

[8] R. Lum and L.O. Chua, Global properties of continuous piecewise linear vector fields. Part I: Simplest case in $\mathbb{R}^2$, Intern. J. Circuit Theory and Appl. **19** (1991), 251–307.

[9] R. Lum and L.O. Chua, Global properties of continuous piecewise linear vector fields. Part II: Simplest symmetric case in $\mathbb{R}^2$, Intern. J. Circuit Theory and Appl. **20** (1992), 9–46.

[10] O. Makarenkov and J.S.W. Lamb, *Dynamics and bifurcations of nonsmooth systems: A survey*, Physica D **241** (2012), 1826–1844.

[11] L. Markus, *Global structure of ordinary differential equations in the plane:* Trans. Amer. Math Soc. **76** (1954), 127–148.

[12] D. A. Neumann, *Classification of continuous flows on 2–manifolds*, Proc. Amer. Math. Soc. **48** (1975), 73–81.

[13] M.M. Peixoto, *On the classification of flows on 2–manifolds*. Academic, New York, pages 389–419, 1973. Dynamical systems (Proc. Sympos., Univ. Bahia, Salvador, 1971).

[14] H. Poincaré, *Mémoire sur les courbes définies par les équations différentielles*, Journal de Mathématiques **37** (1881), 375–422; Oeuvres de Henri Poincaré, vol. I, Gauthier-Villars, Paris, 1951, pp 3–84.

[15] D.J.W. Simpson, *Bifurcations in Piecewise–Smooth Continuous Systems*, World Scientific Series on Nonlinear Science A, vol **69**, World Scientific, Singapore, 2010.

[1] Department of Mathematics, Sichuan University, 610064 Chengdu, Sichuan, P.R. China

E-mail address: `li_jie_math@sina.cn,li_jie_math@126.com`

[2] Departament de Matemàtiques, Universitat Autònoma de Barcelona, 08193 Bellaterra, Barcelona, Catalonia, Spain

E-mail address: `jllibre@mat.uab.cat`

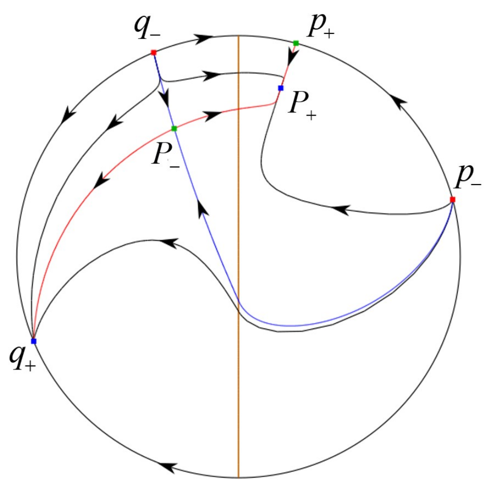

FIGURE 7. $S = 15, R = 4$.

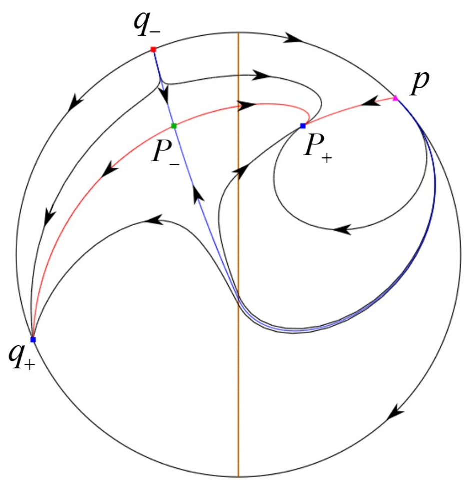

FIGURE 8. $S = 13, R = 4$.

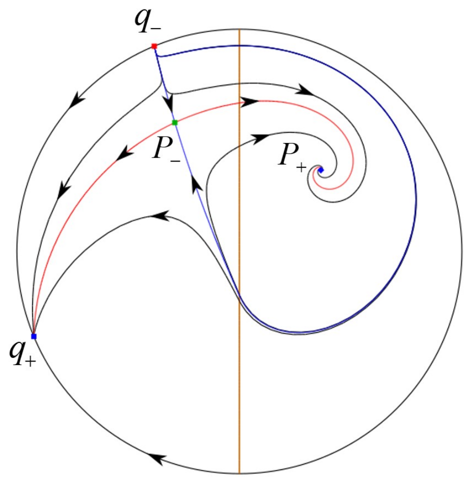

FIGURE 9. $S = 10, R = 3$.

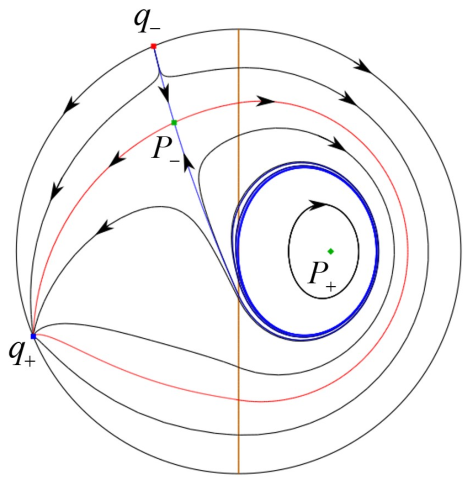

FIGURE 10. $S = 11, R = 4$.

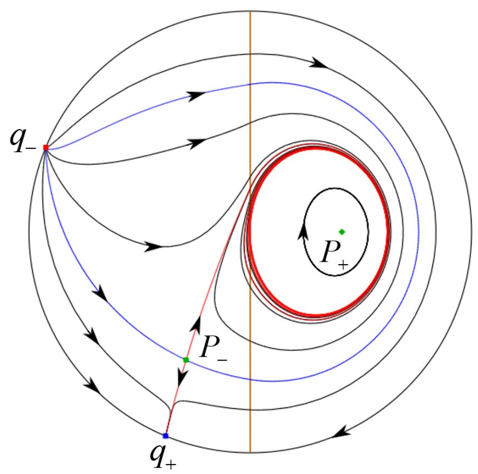

FIGURE 11. $S = 11, R = 4$.

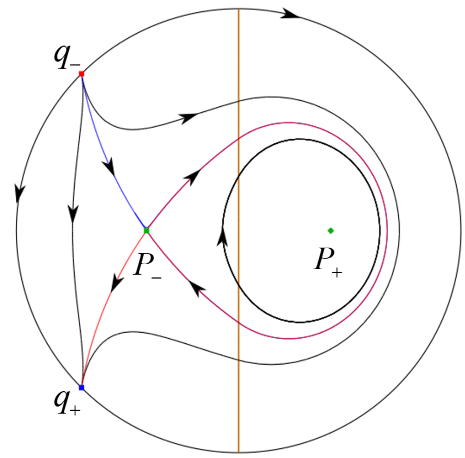

FIGURE 12. $S = 10, R = 3$.

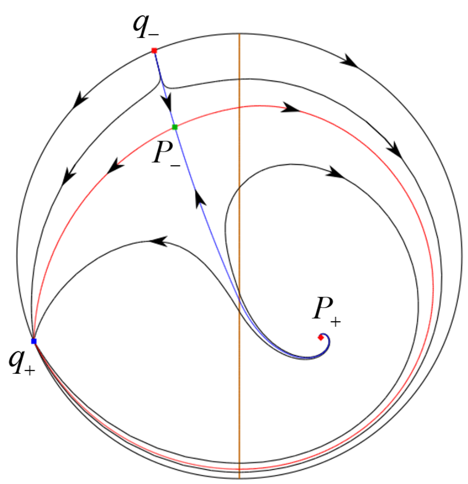

FIGURE 13. $S = 10, R = 3$.

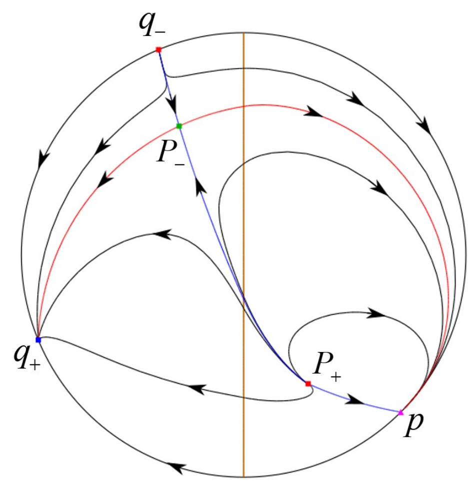

FIGURE 14. $S = 13, R = 4$.

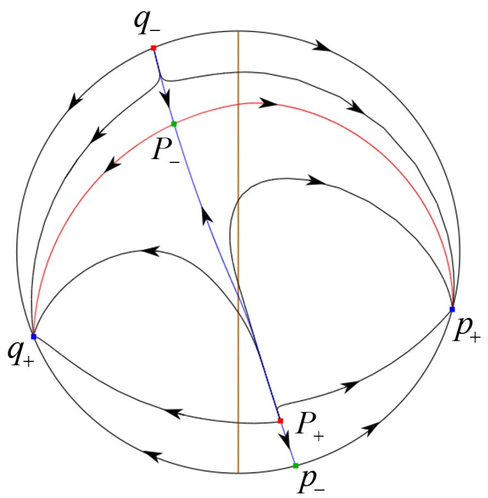

FIGURE 15. $S = 15, R = 4$.

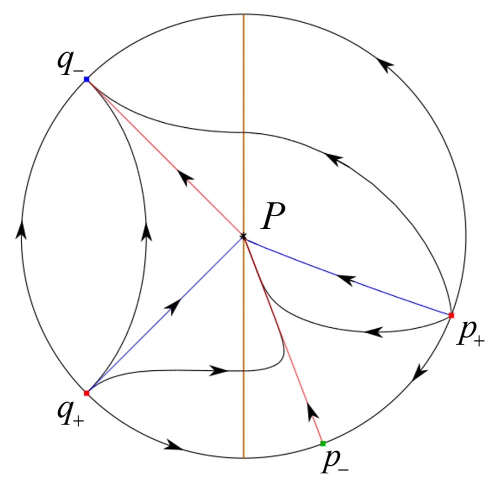

FIGURE 16. $S = 13, R = 4$.

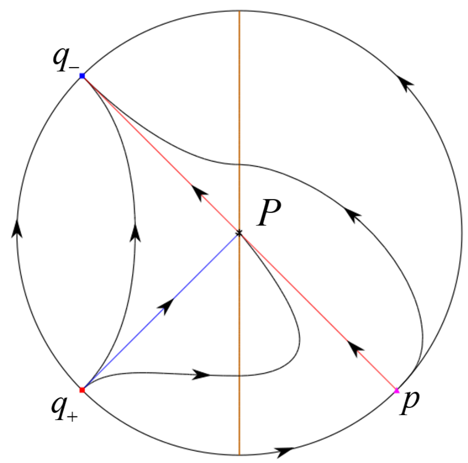

FIGURE 17. $S = 10, R = 3$.

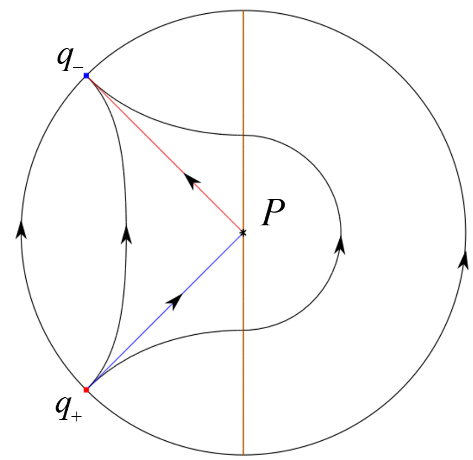

FIGURE 18. $S = 7, R = 2$.

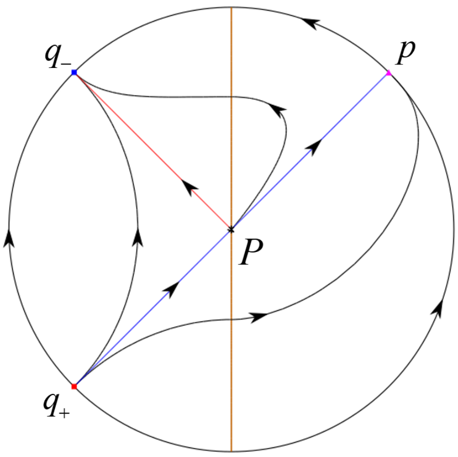

FIGURE 19. $S = 10, R = 3$.

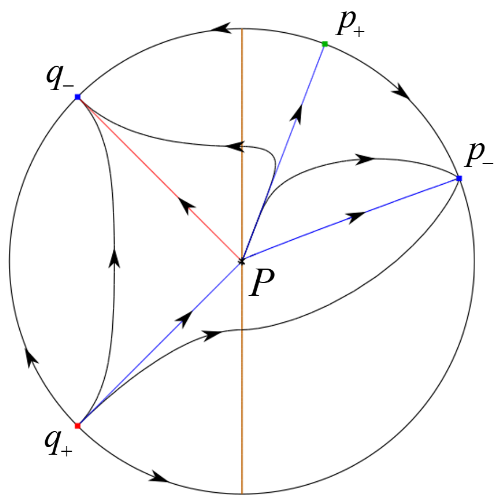

FIGURE 20. $S = 13, R = 4$.

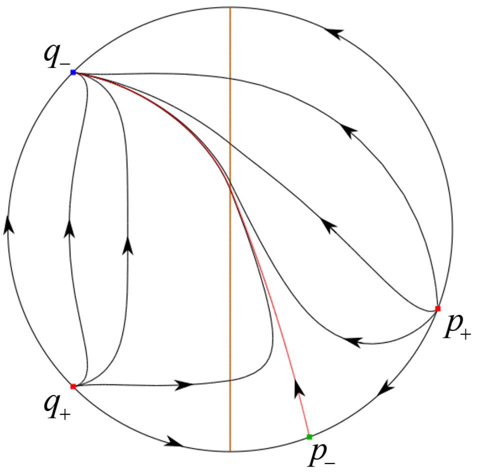

FIGURE 21. $S = 9, R = 2$.

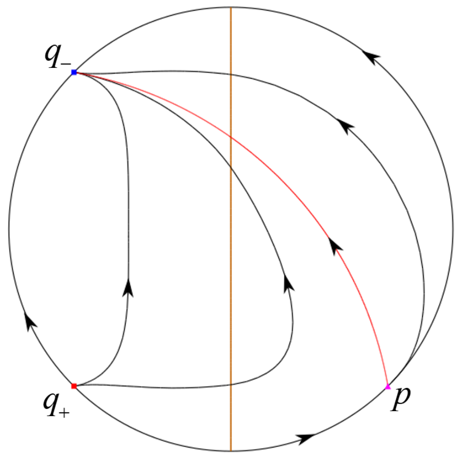

FIGURE 22. $S = 7, R = 2$.

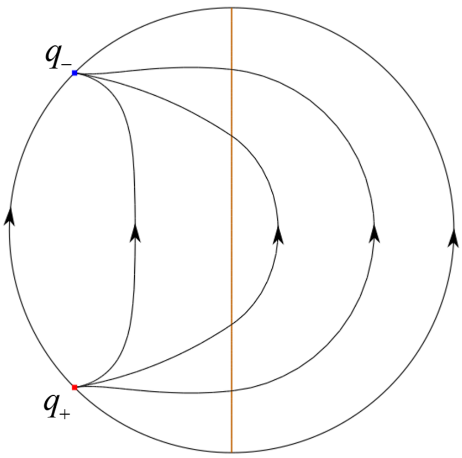

FIGURE 23. $S = 9, R = 1$.

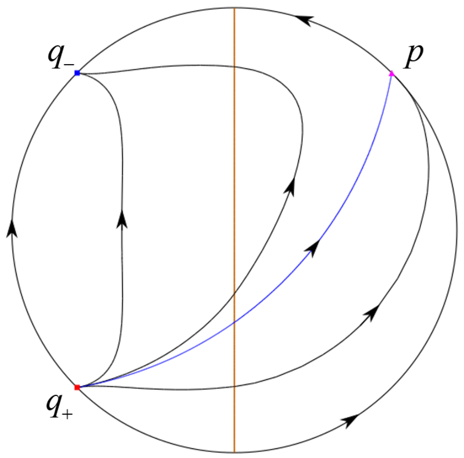

FIGURE 24. $S = 7, R = 2$.

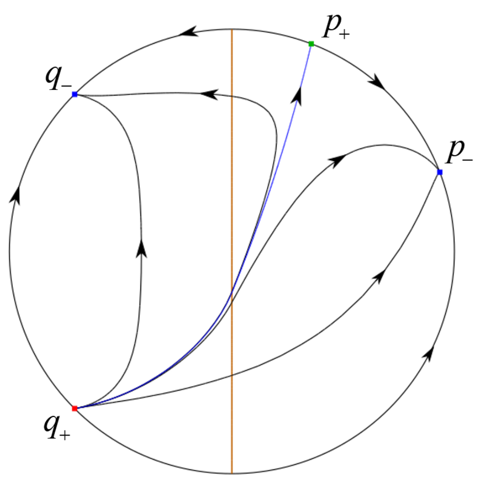

FIGURE 25. $S = 9, R = 2$.

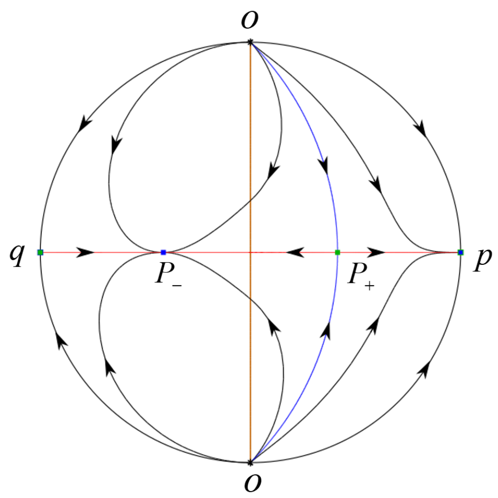

FIGURE 26. $S = 15, R = 4$.

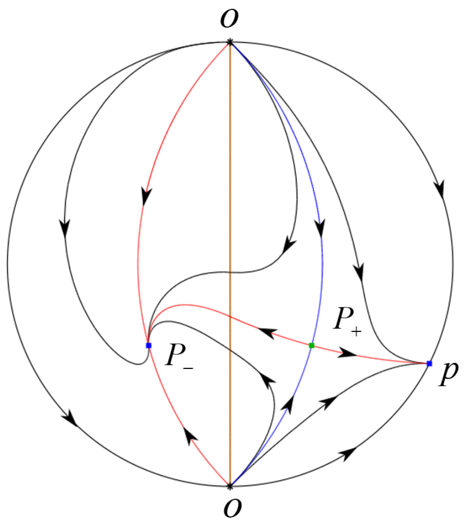

FIGURE 27. $S = 13, R = 4$

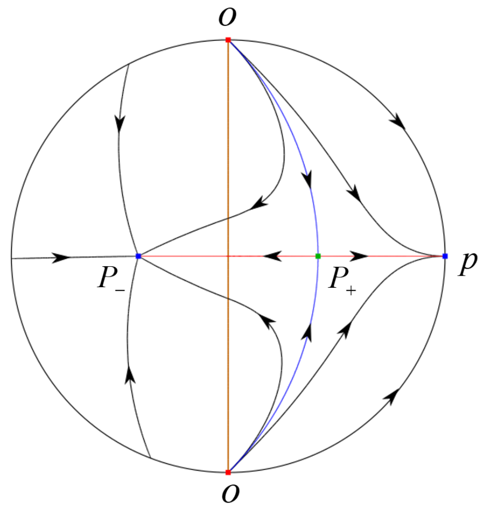

FIGURE 28. $S = \infty$.

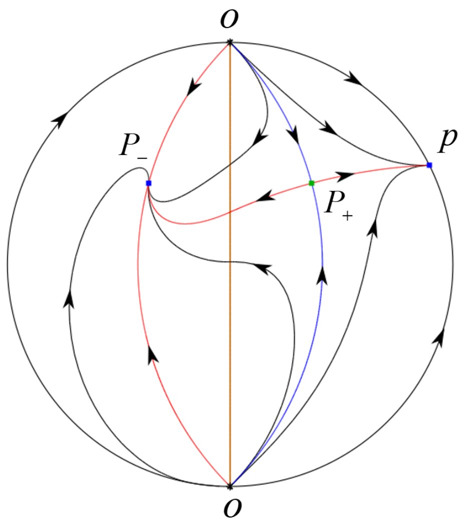

FIGURE 29. $S = 13, R = 4$.

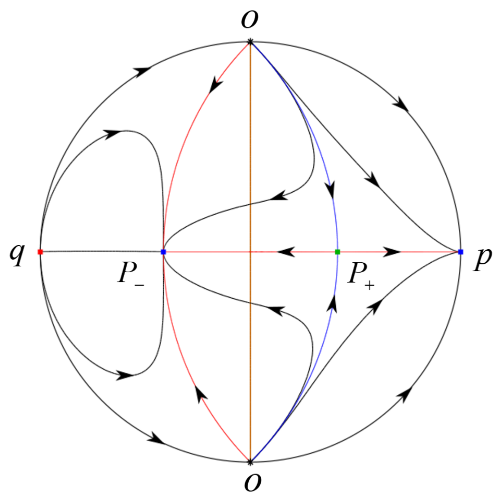

FIGURE 30. $S = 16, R = 5$.

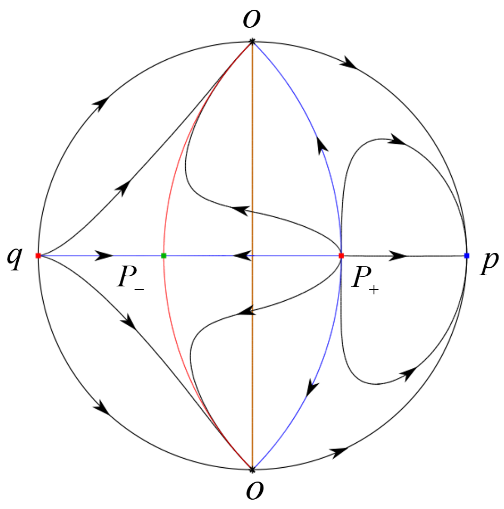

FIGURE 31. $S = 16, R = 5$.

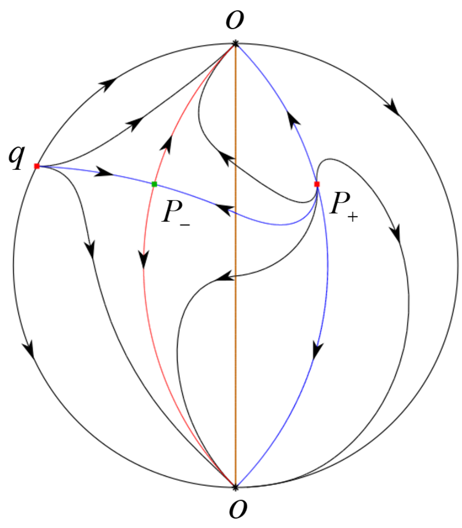

FIGURE 32. $S = 13, R = 4$.

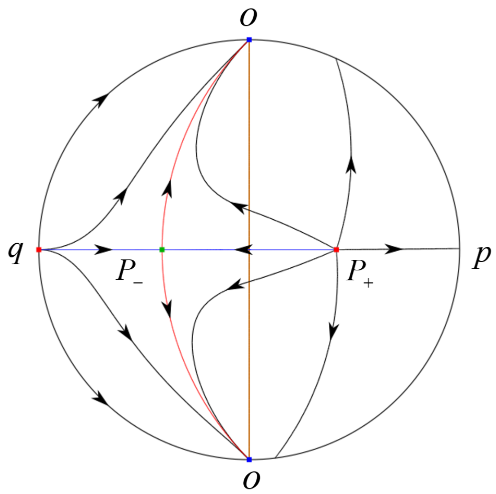

FIGURE 33. $S = \infty$.

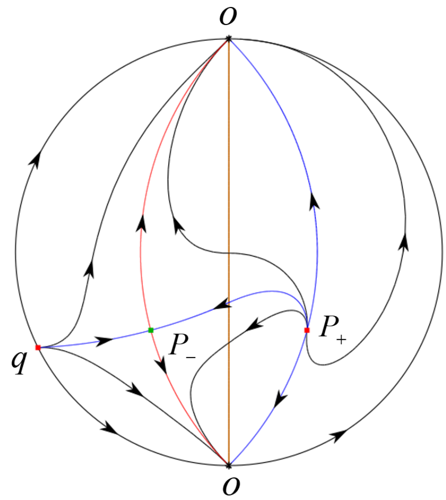

FIGURE 34. $S = 13, R = 4$.

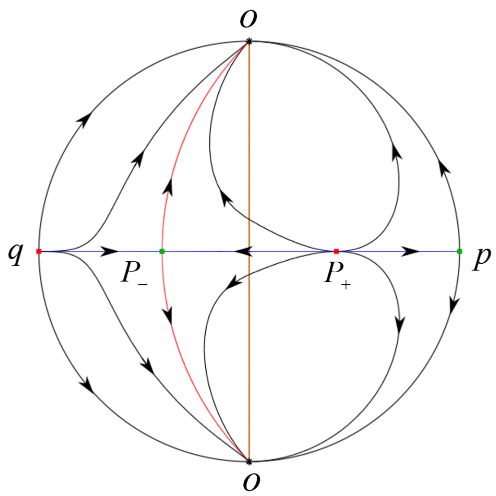

FIGURE 35. $S = 15, R = 4$.

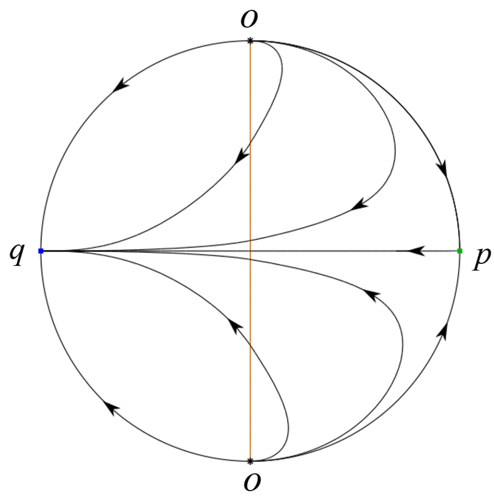

FIGURE 36. $S = 9, R = 2$.

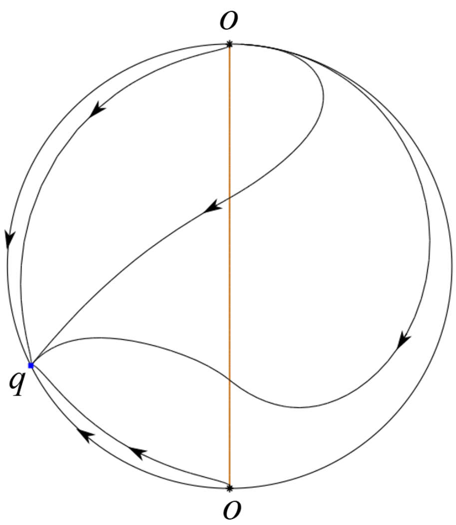

FIGURE 37. $S = 7, R = 2$.

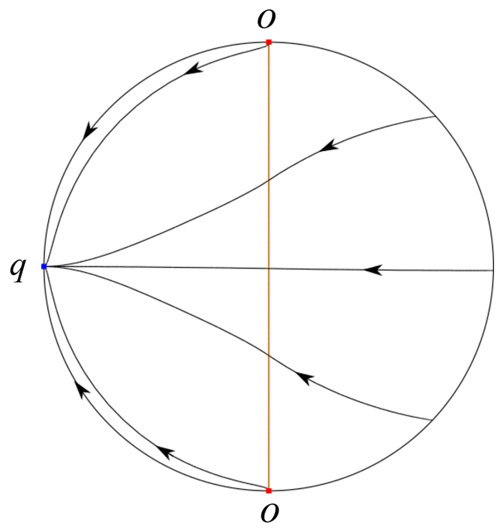

FIGURE 38. $S = \infty$.

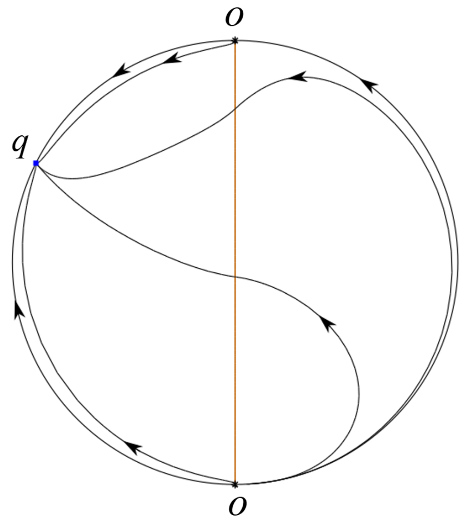

FIGURE 39. $S = 7, R = 2$.

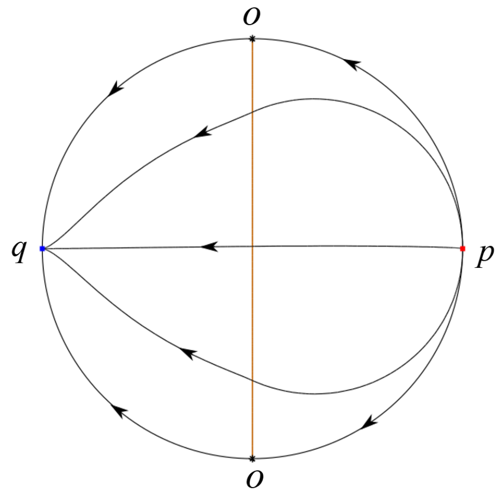

FIGURE 40. $S = 10, R = 3$.

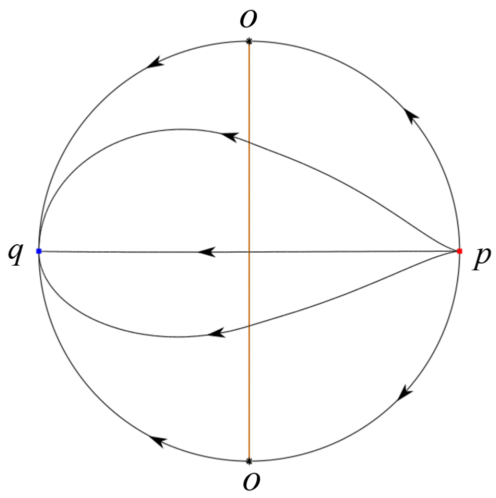

FIGURE 41. $S = 10, R = 3$.

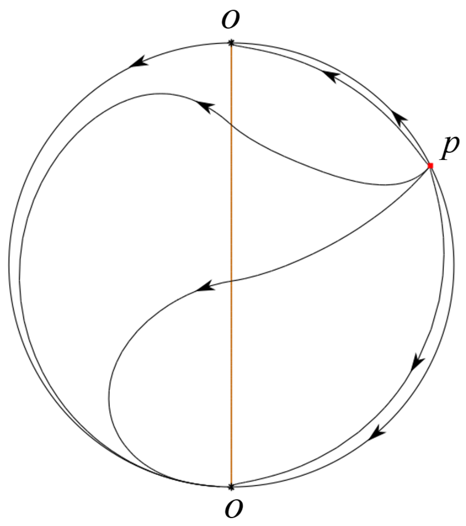

FIGURE 42. $S = 7, R = 2$.

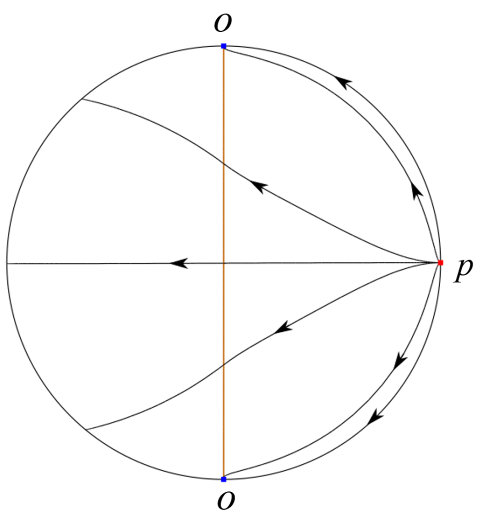

FIGURE 43. $S = \infty$.

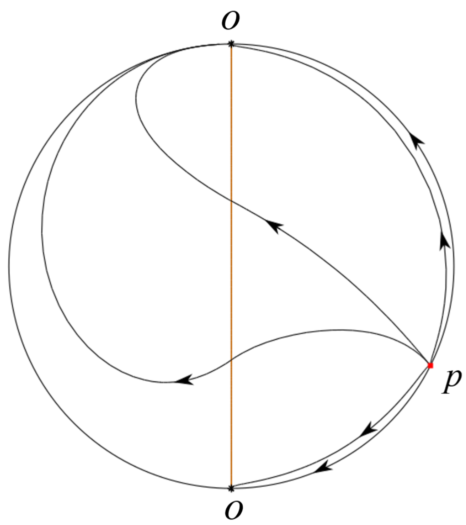

FIGURE 44. $S = 7, R = 2$.

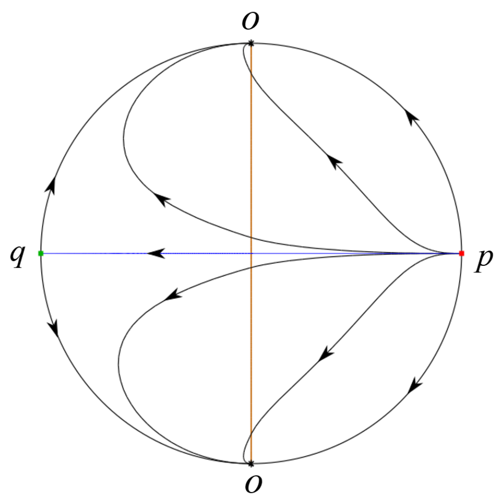

FIGURE 45. $S = 9, R = 2$.

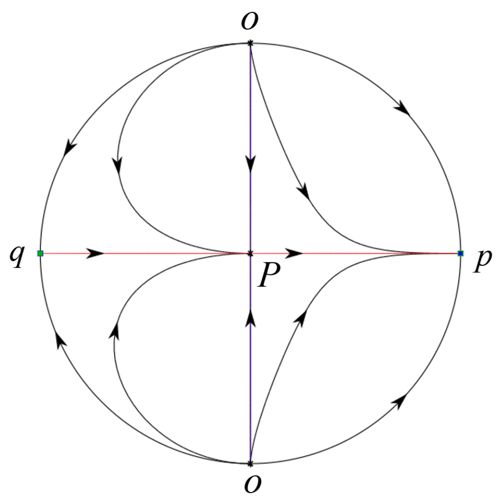

FIGURE 46. $S = 13, R = 4$.

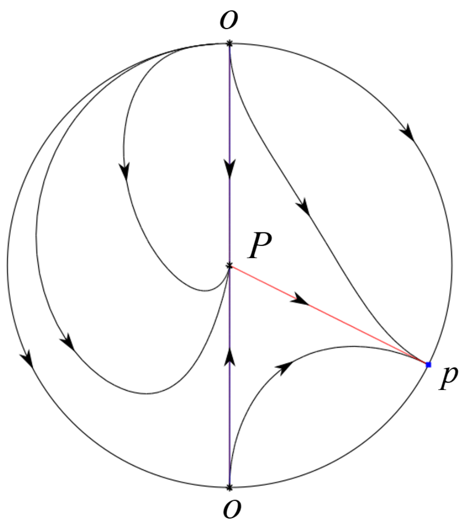

FIGURE 47. $S = 10, R = 3$.

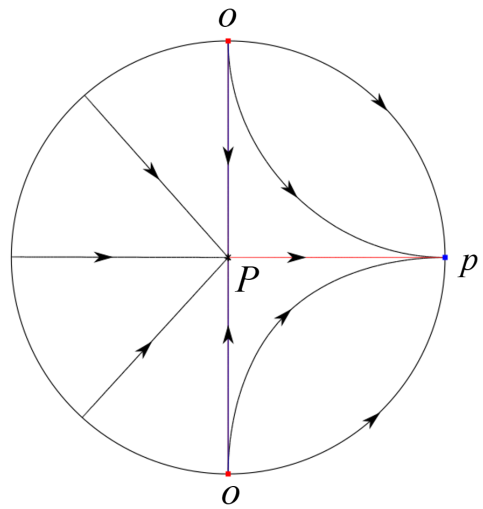

FIGURE 48. $S = \infty$.

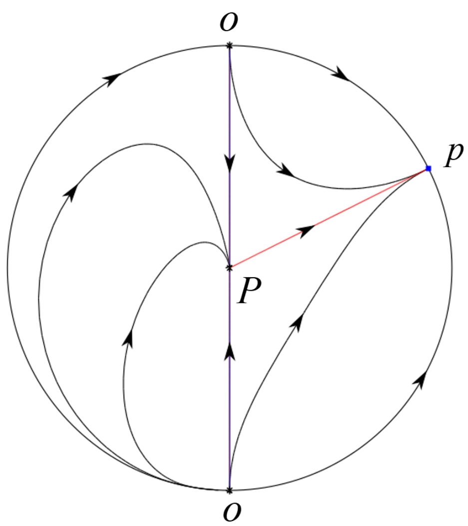

FIGURE 49. $S = 10, R = 3$.

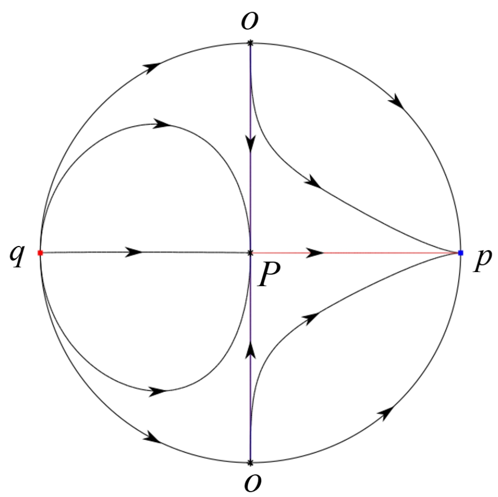

FIGURE 50. $S = 12, R = 3$.

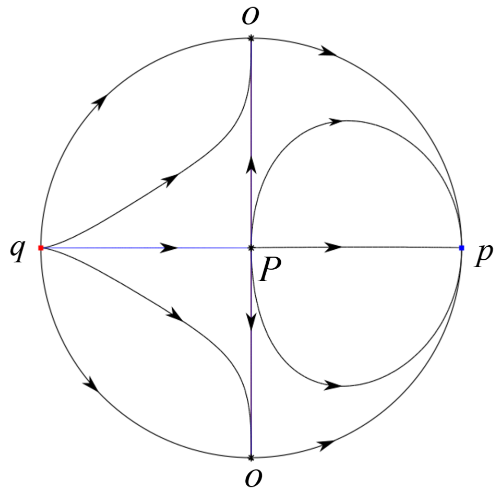

FIGURE 51. $S = 12, R = 3$.

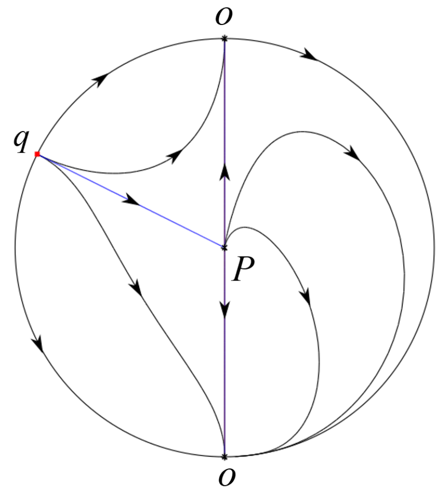

FIGURE 52. $S = 10, R = 3$.

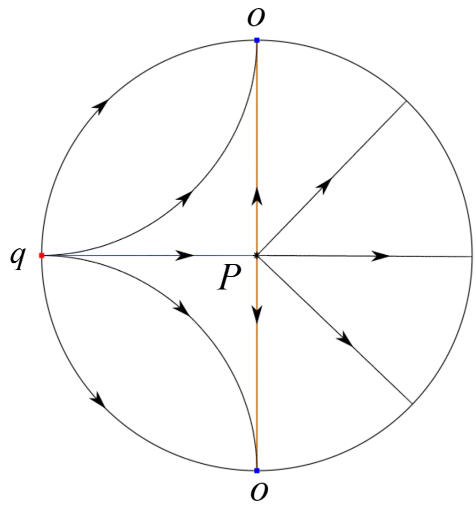

FIGURE 53. $S = \infty$.

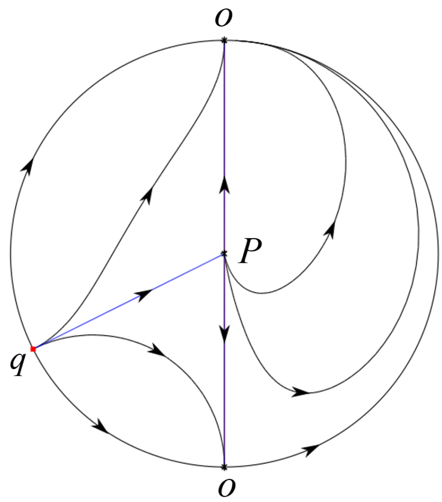

FIGURE 54. $S = 10, R = 3$.

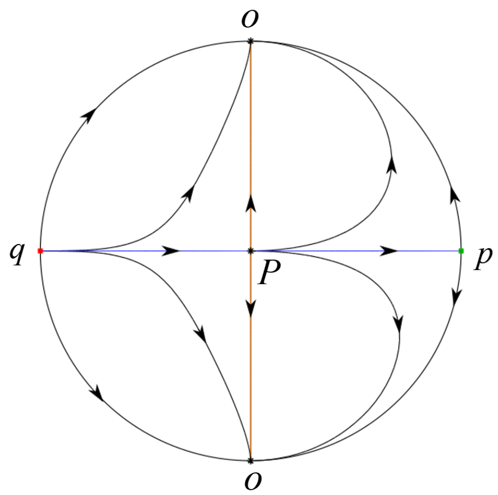

FIGURE 55. $S = 13, R = 4$.